Inorganic Chemistry

Article

pubs.acs.org/IC

# Chloro- and Trifluoromethyl-Substituted Flanking-Ring *m*-Terphenyl Isocyanides: $\eta^6$-Arene Binding to Zero-Valent Molybdenum Centers and Comparison to Alkyl-Substituted Derivatives

Treffly B. Ditri, Alex E. Carpenter, Donald S. Ripatti, Curtis E. Moore, Arnold. L. Rheingold, and Joshua S. Figueroa*

Department of Chemistry and Biochemistry, University of California, San Diego, 9500 Gilman Drive, Mail Code 0358, La Jolla, California 92093-0358, United States

Supporting Information

**ABSTRACT:** Presented herein are synthetic and structural studies exploring the propensity of *m*-terphenyl isocyanide ligands to provide flanking-ring $\eta^6$-arene interactions to zerovalent molybdenum centers. The alkyl-substituted *m*-terphenyl isocyanides $CNAr^{Mes2}$ and $CNAr^{Dipp2}$ ($Ar^{Mes2}$ = 2,6-(2,4,6-$Me_3C_6H_2)_2C_6H_3$; $Ar^{Dipp2}$ = 2,6-(2,6-(*i*-Pr)$_2C_6H_3)_2C_6H_3$) react with Mo($\eta^6$-napthalene)$_2$ in a 3:1 ratio to form tris-isocyanide $\eta^6$-arene Mo complexes, in which a flanking mesityl or 2,6-diisopropylphenyl group, respectively, of one isocyanide ligand is bound to the zerovalent molybdenum center. Thermal stability and reactivity studies show that these flanking ring $\eta^6$-arene interactions are particularly robust. To weaken or prevent formation of a flanking-ring $\eta^6$-arene interaction, and to potentially provide access to the coordinatively unsaturated [Mo($CNAr^R$)$_3$] fragment, the new halo-substituted *m*-terphenyl isocyanides $CNAr^{Clips2}$ and $CNAr^{DArF2}$ ($Ar^{Clips}$ = 2,6-(2,6-$Cl_2C_6H_3)_2$(4-*t*-Bu)$C_6H_2$; $Ar^{DArF2}$ = 2,6-(3,5-$(CF_3)_2C_6H_3)_2C_6H_3$) have been prepared. Relative to their alkyl-substituted counterparts, synthetic and structural studies demonstrate that the flanking aryl rings of $CNAr^{Clips2}$ and $CNAr^{DArF2}$ display a lower tendency toward $\eta^6$-binding. In the case of $CNAr^{DArF2}$, it is shown that an $\eta^6$-bound 3,5-bis(trifluoromethyl)phenyl group can be displaced from a zerovalent molybdenum center by three molecules of acetonitrile. This observation suggests that the $CNAr^{DArF2}$ ligand effectively masks low-valent metal centers in a fashion that provides access to low-coordinate isocyano targets such as [Mo($CNAr^R$)$_3$]. A series of Mo(CO)$_3$($CNAr^R$)$_3$ complexes were also prepared to compare the relative $\pi$-acidities of $CNAr^{Mes2}$, $CNAr^{Clips2}$, and $CNAr^{DArF2}$. It is found that $CNAr^{DArF2}$ shows increased $\pi$-acidity relative to $CNAr^{Mes2}$ and $CNAr^{Clips2}$, despite the fact that its electron-withdrawing $CF_3$ groups are fairly distal to the terminal isocyano unit.


## INTRODUCTION

Over the past two decades, the *m*-terphenyl group has become an important and extensively utilized ancillary framework for the stabilization of low-coordinate transition-metal and main-group complexes.[1−11] The appeal of the *m*-terphenyl framework as a ligand is derived from its ability to foster an encumbering and protective environment around a central atom or group of atoms. It has also found wide use because of the relative ease with which the steric properties of its framework can be modified. Whereas $\sigma$-aryl *m*-terphenyl derivatives are convenient to prepare and have been broadly employed,[1−10] it is important to note that a variety of donor atoms and groups have also been appended to the central framework ring to provide altered ligation properties. Accordingly, *m*-terphenyl-based aryloxides,[12−16] thiolates,[17−20] amidos,[21−29] imidos,[30,31] and carboxylates,[32−38] have all been reported as ancillary ligands for either transition-metal or main-group systems. Our group has used the *m*-terphenyl framework in conjunction with the isocyanide functionality (CNR) in an effort to study a class of encumbering ligands that mimic the electronic properties of carbon monoxide (CO).[39−43] We have used these ligands for the generation of low-coordinate isocyanide complexes that are reminiscent of the binary unsaturated transition-metal carbonyls (e.g., Co(CO)$_4$, Ni(CO)$_3$, and Pd(CO)$_2$).[44−47]

During our studies of cobalt complexes supported by the *m*-terphenyl isocyanide ligand $CNAr^{Mes2}$ ($Ar^{Mes2}$ = 2,6-(2,4,6-$Me_3C_6H_2)_2C_6H_3$), we uncovered that the flanking mesityl rings of this ligand could provide a robust $\eta^6$-arene interaction to low-valent cobalt centers.[48] Formation of this interaction clearly results as an effort to maximize coordinative saturation, especially in very low-coordinate environments. However, when coordinatively unsaturated metal centers are the intended synthetic targets, the propensity of the *m*-terphenyl framework to engage in $\eta^6$-arene coordination is an undesirable property.

**Received:** August 24, 2013
**Published:** October 30, 2013

   dx.doi.org/10.1021/ic402130p | *Inorg. Chem.* 2013, 52, 13216−13229

Notably, "$\eta^6$-arene capping" of low-coordinate metal fragments by flanking rings has been observed by Power, Dilworth, Rothwell, and others for $\sigma$-aryl,[49,50] amido,[25] thiolate,[51−54] aryloxide,[55−58] phosphine,[59] and acetylene[60] *m*-terphenyl-based ligands. In these examples, the $\eta^6$-bound flanking arene rings are unsubstituted ($C_6H_5$) or feature 2,4,6-trimethyl (i.e., mesityl; Mes = 2,4,6-$Me_3C_6H_2$), 2,6-diisopropyl (i.e., Dipp = 2,6-$(i\text{-}Pr)_2C_6H_3$) or 2,4,6- triisopropyl (i.e., Tripp = 2,4,6-$(i\text{-}Pr)_3C_6H_2$) substitution patterns.

As an attempt to circumvent this problem, we reasoned that electron-withdrawing substituents on the flanking aryl rings of the *m*-terphenyl framework might provide a sufficiently deactivated arene system to resist $\eta^6$-coordination to low-coordinate and low-valent metal centers. This idea stems from the fact that electron-deficient arenes are well-known to foster kinetically labile $\eta^6$ interactions to low-valent, middle d-block transition metals.[61−69] This behavior is especially pronounced when compared to arenes possessing electron-releasing alkyl groups. Furthermore, *m*-terphenyl groups featuring electron withdrawing substituents on the flanking rings are not common in coordination chemistry,[70,71] which warranted their synthesis and incorporation into an *m*-terphenyl isocyanide ligand. Such derivatives would additionally provide an important steric and electronic comparison to the alkyl-substituted *m*-terphenyl isocyanides $CNAr^{Mes2}$ and $CNAr^{Dipp2}$ ($Ar^{Dipp2}$ = 2,6-(2,6-$(i\text{-}Pr)_2C_6H_3)_2C_6H_3$).[40,42,43] Presented in this report are the syntheses of the halo-substituted *m*-terphenyl isocyanide ligands, $CNAr^{Clips2}$ ($Ar^{Clips2}$ = 2,6-$(2,6\text{-}Cl_2C_6H_3)_2$(4-*t*-Bu)-$C_6H_2$)[72] and $CNAr^{DArF2}$ ($Ar^{DArF2}$ = 2,6-$(3,5\text{-}(CF_3)_2C_6H_3)_2C_6H_3$), and a demonstration of their coordination behavior toward zerovalent molybdenum centers. Furthermore, the abilities of $CNAr^{Clips2}$ and $CNAr^{DArF2}$ to foster a flanking-arene $\eta^6$-interaction are compared with those of $CNAr^{Mes2}$ and $CNAr^{Dipp2}$. While these halo-substituted *m*-terphenyls can bind in an $\eta^6$-fashion, the formation of such interactions is significantly less facile than for their alkyl-substituted counterparts. In addition, $\eta^6$-interactions from halo-substituted *m*-terphenyls are found to be fairly labile in some cases and therefore may be considered a potentially effective "masking" strategy for reactive, low-valent metal centers.

## RESULTS AND DISCUSSION

**1. Flanking-Ring Binding of the Isocyanides $CNAr^{Dipp2}$ and $CNAr^{Mes2}$ to Zerovalent Molybdenum.** In a previous study, we reported our efforts to generate the two-coordinate molybdenum bis-isocyanide complex $[Mo(CNAr^{Dipp2})_2]$ through a tandem oxidative-decarbonylation/reduction synthetic sequence.[43] This approach was not successful for its intended target. Instead, zerovalent, bis-isocyanide-$\eta^6$-arene complexes of molybdenum were isolated when the reduction step was carried out in arene solvents, whereas intractable mixtures were produced when chemical reductions were performed in higher-polarity solvents such as $Et_2O$ or tetrahydrofuran (THF). These observations, and the operational inconvenience of the tandem oxidative-decarbonylation/reduction sequence, prompted us to find a more direct synthetic route to low-coordinate, zerovalent molybdenum *m*-terphenyl isocyanide complexes. Accordingly, we turned to molybdenum bis-naphthalene ($Mo(\eta^6\text{-}C_{10}H_8)_2$) as a synthetic precursor,[73] as this complex has been shown to serve as a source of zerovalent molybdenum upon reaction with monodentate neutral donor ligands such as isocyanides and phosphines ($PR_3$).[74,75]

Treatment of a benzene solution of $Mo(\eta^6\text{-}C_{10}H_8)_2$ with 3.0 equiv of $CNAr^{Dipp2}$ proceeds to the tris-isocyanide, $\eta^6$-arene complex $Mo(\eta^6\text{-(Dipp)-}\kappa^1\text{-C-}CNAr^{Dipp})(CNAr^{Dipp2})_2$ ($\mathbf{1}^{Dipp}$) with the loss of 2 equiv of naphthalene (Scheme 1). Addition

**Scheme 1**

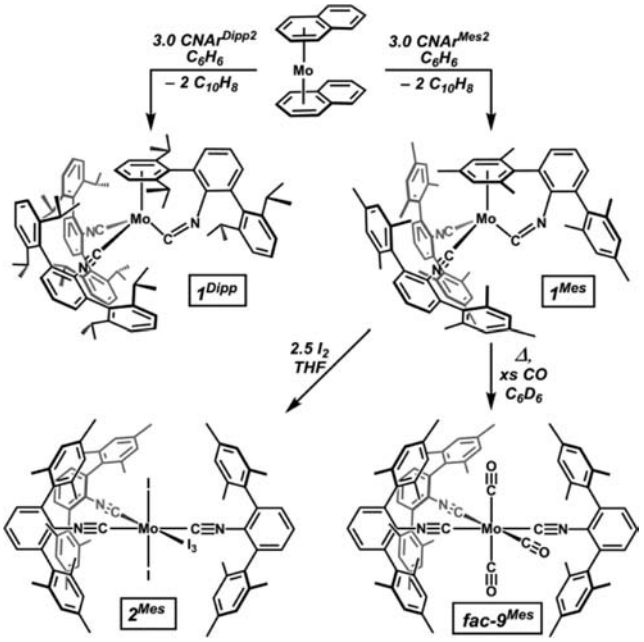


of 3.0 equiv of the less encumbering isocyanide $CNAr^{Mes2}$ to $Mo(\eta^6\text{-}C_{10}H_8)_2$ in benzene similarly produces $Mo(\eta^6\text{-(Mes)-}\kappa^1\text{-C-}CNAr^{Mes})(CNAr^{Mes2})_2$ ($\mathbf{1}^{Mes}$, Scheme 1), which possesses an $\eta^6$-bound mesityl ring. The $^1$H NMR spectra of $\mathbf{1}^{Dipp}$ and $\mathbf{1}^{Mes}$ exhibit an overall $C_s$-symmetric pattern of $Ar^{R2}$ residues and upfield-shifted arene resonances consistent with the $\eta^6$-binding of a single *m*-terphenyl flanking ring. Structural characterization of both $\mathbf{1}^{Dipp}$ and $\mathbf{1}^{Mes}$ (Figures 1−2) revealed that each adopts the three-legged piano stool motif typical for Group-6 metal ($\eta^6$-arene)$ML_3$ complexes. However, $\mathbf{1}^{Dipp}$ and $\mathbf{1}^{Mes}$ are unique with respect to the geometric constraints that $\eta^6$-binding of the flanking-arene ring places on the isocyanide unit to which it is attached. As shown in Figures 1 and 2, $\eta^6$-binding of either a Dipp or Mes ring results in significantly bent $C_{iso}$−N−$C_{ipso}$ angles of 120.3(6)° and 120.52(16)° in $\mathbf{1}^{Dipp}$ and $\mathbf{1}^{Mes}$, respectively. According to the Cambridge Structural Database,[76] these values represent the most acute $C_{iso}$−N−C angles for structurally characterized isocyanide complexes to date.[77] The geometrically constrained isocyanide ligands in $\mathbf{1}^{Dipp}$ and $\mathbf{1}^{Mes}$ also feature greatly elongated isocyanide C−N bond lengths of 1.244(9) Å and 1.244(2) Å, respectively, and display very low energy $\nu_{CN}$ bands of 1652 $cm^{-1}$ and 1643 $cm^{-1}$, respectively, in their IR spectra (Table 1). Importantly, we believe these structural and spectroscopic properties result from a disruption of N→C $\pi$-donation, rather than from significant M→ligand $\pi$ back-donation, as a consequence of the geometric constraints placed on the isocyanide by flanking-ring $\eta^6$-binding. These observations, and the fact that the constrained $C_{iso}$ atoms in $\mathbf{1}^{Dipp}$ and $\mathbf{1}^{Mes}$ give rise to very large downfield chemical shifts ($\mathbf{1}^{Dipp}$ $\delta$ = 281.6 ppm ($C_6D_6$); $\mathbf{1}^{Mes}$ $\delta$ = 278.0 ppm ($C_6D_6$)), suggest that $\eta^6$-arene tethering imparts significant and static carbenic character on the isocyanide carbon of these ligands.[78]


dx.doi.org/10.1021/ic402130p | *Inorg. Chem.* 2013, 52, 13216−13229

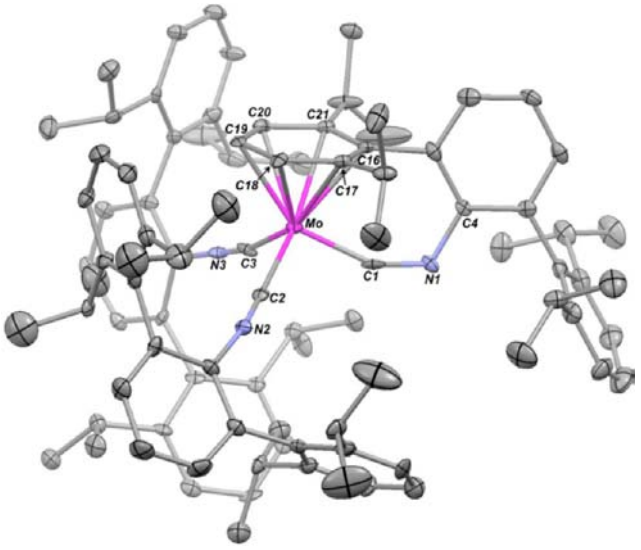


**Figure 1.** Molecular structure of Mo($\eta^6$-(Dipp)-$\kappa^1$-C-CNAr$^{Dipp}$)-(CNAr$^{Dipp2}$)$_2$ (**1**$^{Dipp}$). Selected bond distances (Å) and angles (deg): Mo1−C1 = 1.939(8); Mo1−C2 = 2.042(6); Mo1−C3 = 2.060(7); Mo1−C16 = 2.317(6); Mo1−C17 = 2.361(6); Mo1−C18 = 2.295(6); Mo1−C19 = 2.329(6); Mo1−C20 = 2.296(6); Mo1−C21 = 2.346(5); C1−N1 = 1.244(9); N1−C4 = 1.417(7); Mo1−C1−N1 = 155.3(5); C1−N1−C4 = 120.3(6).

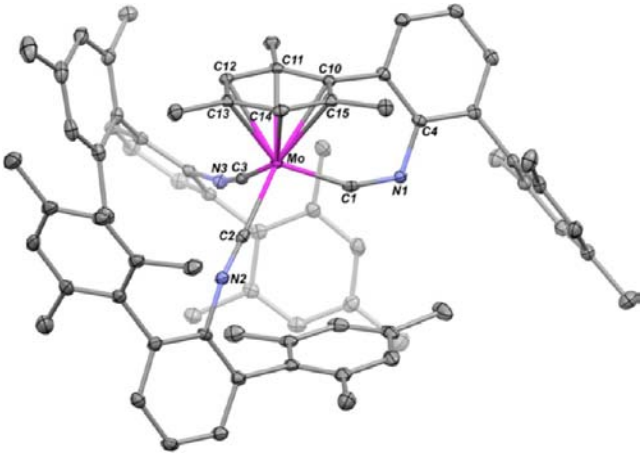


**Figure 2.** Molecular structure of Mo($\eta^6$-(Mes)-$\kappa_1$-C−CNAr$^{Mes}$)-(CNAr$^{Mes2}$)$_2$ (**1**$^{Mes}$). Selected bond distances (Å) and angles (deg): Mo1−C1 = 1.9360(19); Mo1−C2 = 2.0457(19); Mo1−C3 = 2.0045(19); Mo1−C10 = 2.3061(18); Mo1−C11 = 2.3225(18); Mo1−C12 = 2.3133(19); Mo1−C13 = 2.3424(18); Mo1−C14 = 2.3596(18); Mo1−C15 = 2.3667(18); C1−N1 = 1.244(2); N1−C4 = 1.414(2); C1−Mo1−C2 = 102.09(7); Mo1−C1−N1 = 152.63(15); C1−N1−C4 = 120.52(16).

It is important to note that the flanking-ring $\eta^6$-arene interactions in **1**$^{Dipp}$ and **1**$^{Mes}$ readily form despite the use of benzene as a solvent. In addition, these $\eta^6$-arene interactions in **1**$^{Dipp}$ and **1**$^{Mes}$ cannot be displaced by external arene substrates after synthesis. For example, incorporation of benzene or toluene does not take place when pure **1**$^{Dipp}$ and **1**$^{Mes}$ are heated in these solvents up to 120 °C for several days. The observation that benzene or toluene does not displace the substituted $\eta^6$-arene ligands in **1**$^{Dipp}$ and **1**$^{Mes}$ is consistent with findings that electron-rich arene ligands foster more thermodynamically stable $\eta^6$-arene interactions to transition metal fragments than electron deficient arenes.[61−69] In the case of **1**$^{Mes}$, the $\eta^6$-arene interaction can be disrupted oxidatively by excess $I_2$ to form the $d^3$ diiodo-triiodide complex *mer*-MoI$_2$(I$_3$)(CNAr$^{Mes2}$)$_3$ (**2**$^{Mes}$; Scheme 2, Figure 3) or by treatment with an excess of CO under forcing conditions (100 °C, 5d) to form *mer*-Mo(CO)$_3$(CNAr$^{Mes2}$)$_3$.[40] Neither **1**$^{Dipp}$ nor **1**$^{Mes}$ react with $H_2$, $H_2O$, or additional isocyanide ligand in benzene solution at elevated temperatures over the course of several days. The complexes also do not react with the coordinating solvents NCMe or THF at room temperature or above.

**2. Synthesis of the Halo-Substituted Isocyanide Ligands CNAr$^{Clips2}$ and CNAr$^{DArF2}$.** Despite possessing the empirical formula Mo(CNR)$_3$, the robust $\eta^6$-arene interactions in **1**$^{Dipp}$ and **1**$^{Mes}$ do not allow these complexes to serve as structural or functional mimics of the reactive binary carbonyl species [Mo(CO)$_3$].[79−81] To weaken, or ideally prevent, $\eta^6$-arene interactions, we sought to synthetically append electron-withdrawing substituents, such as halides, to the flanking ring of the *m*-terphenyl isocyanide framework. Halo-substituted *m*-terphenyl groups are uncommon, especially for substitution in the flanking rings. However, Protasiewicz has reported the synthesis of the 2,6-dichlorophenyl substituted *m*-terphenyl group 2,6-(2,6-Cl$_2$C$_6$H$_3$)$_2$C$_6$H$_3$ for the preparation of sterically protected diphosphenes.[70b] Inspired by this report, we prepared the modified 2,6-dichlorophenyl-substituted *m*-terphenyl isocyanide CNAr$^{Clips2}$ from 2,6-(2,6-Cl$_2$C$_6$H$_3$)$_2$C$_6$H$_3$I in five steps as outlined in Scheme 2. At the *m*-terphenyl iodide stage, a *para-tert*-butyl group was installed on the ligand framework via Friedel−Crafts alkylation to promote solubility and crystallinity, as well as to provide a convenient $^1$H NMR handle. The free CNAr$^{Clips2}$ isocyanide is characterized by $\nu_{CN}$ stretch of 2132 cm$^{-1}$ (KBr) and a C$_{iso}$ $^{13}$C{$^1$H} NMR chemical shift of $\delta$ = 172.0 ppm (C$_6$D$_6$).

In addition to CNAr$^{Clips2}$, we sought to develop an *m*-terphenyl isocyanide in which the flanking aryl groups were further deactivated toward $\eta^6$-binding by the presence of trifluoromethyl (CF$_3$) groups. Accordingly, we targeted the bis-(trifluoromethyl)phenyl substituted isocyanide CNAr$^{DArF2}$ (Scheme 3), which we view as reminiscent of the weakly coordinating tetraarylborate anion [B(3,5-(CF$_3$)$_2$C$_6$H$_3$)$_4$]$^-$ ([BAr$^F_4$]$^-$).[82] Despite the widespread use [BAr$^F_4$]$^-$ as a counterion,[83] $\eta^6$-coordination of one of its 3,5-(CF$_3$)$_2$C$_6$H$_3$ groups to a transition-metal center is currently limited to only two structurally characterized examples.[84,85] As shown in

**Table 1. Spectroscopic and Structural Parameters for the Geometrically-Constrained Isocyanide Ligand in Complexes 1$^R$**

| complex | $\nu_{CN}$[a] (cm$^{-1}$) | $\delta$ C$_{iso}$[a] (ppm) | ∠(C$_{iso}$−N−C$_{ipso}$) (deg) | *d*(C$_{iso}$−N) (Å) |
|---|---|---|---|---|
| Mo($\eta^6$-(Dipp)-$\kappa^1$-C-CNAr$^{Dipp}$)(CNAr$^{Dipp2}$)$_2$ (**1**$^{Dipp}$) | 1652 | 281.6 | 120.3(6) | 1.244(9) |
| Mo($\eta^6$-(Mes)-$\kappa^1$-C-CNAr$^{Mes}$)(CNAr$^{Mes2}$)$_2$ (**1**$^{Mes}$) | 1643 | 278.0 | 120.52(16) | 1.244(2) |
| Mo($\eta^6$-(2,6-Cl$_2$C$_6$H$_3$)-$\kappa^1$-C-CNAr$^{Clips}$)(CNAr$^{Clips2}$)$_2$ (**1**$^{Clips}$) | 1680 | 275.6 | 120.1(2) | 1.235(4) |
| Mo($\eta^6$-(3,5-(CF$_3$)$_2$C$_6$H$_3$)-$\kappa^1$-C-CNAr$^{DArF}$)(CNAr$^{DArF2}$)$_2$ (**1**$^{DArF}$) | 1717 | 273.3 | 120.8(3) | 1.229(4) |

[a]Measured in C$_6$D$_6$ solution.


dx.doi.org/10.1021/ic402130p | *Inorg. Chem.* 2013, 52, 13216−13229

Scheme 2

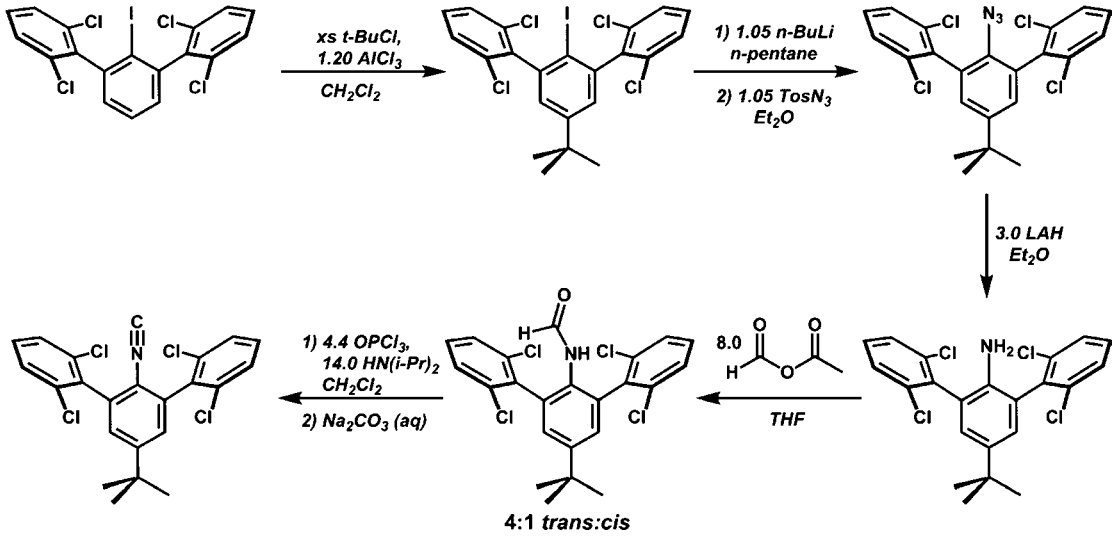


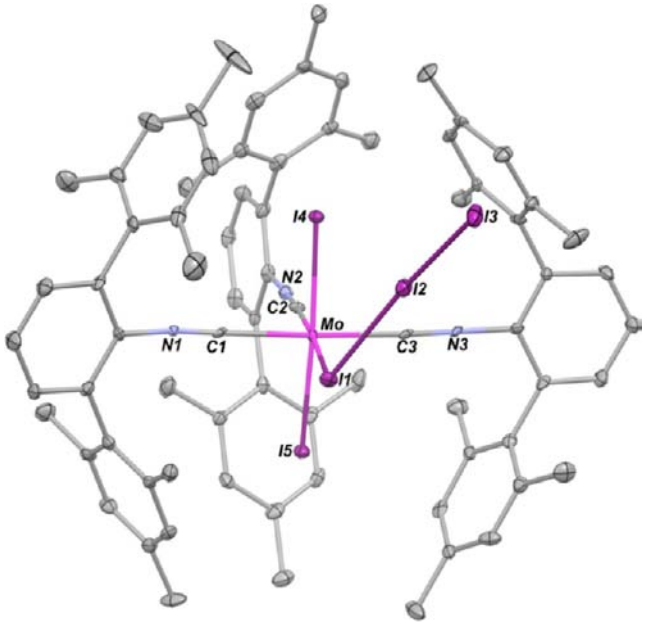


**Figure 3.** Molecular structure of *mer*-$MoI_2(I_3)(CNAr^{Mes2})_3$ ($\mathbf{2}^{Mes}$). Selected bond distances (Å) and angles (deg): Mo1−C1 = 2.173(8); Mo1−C2 = 2.120(9); Mo1−C3 = 2.160(9); Mo1−I1 = 2.7756(9); Mo1−I4 = 2.6813(8); Mo1−I5 = 2.7133(8); C1−Mo1−C2 = 92.5(3); C1−Mo1−C3 = 173.1(3); C1−Mo1−I1 = 85.8(2); C1−Mo1−I4 = 88.1(2); C1−Mo1−I5 = 90.7 (2); C2−Mo1−C3 = 93.2(3); C2−Mo1−I1 = 176.1(2); C2−Mo1−I4 = 88.1(2); C2−Mo1−I5 = 86.3(2); C3−Mo1−I1 = 88.8(2); C3−Mo1−I4 = 89.3 (2); C3−Mo1−I5 = 93.5(2); I1−Mo1−I4 = 95.33(3); I1−Mo1−I5 = 90.26(2); I4−Mo1−I5 = 173.80(3).

Scheme 3, $CNAr^{DArF2}$ is readily synthesized in good overall yield by palladium-catalyzed cross-coupling of 2,6-dibromoaniline with 3,5-$(CF_3)_2C_6H_3B(OH)_2$ and subsequent formylation/dehydration steps. Free $CNAr^{DArF2}$ gives rise to an isocyanide $C_{iso}$ $^{13}C\{^1H\}$ NMR chemical shift of $\delta$ = 175.4 ppm in $C_6D_6$ solution, and its solid-state IR spectrum (KBr) exhibits a $\nu_{CN}$ band at 2119 $cm^{-1}$.

The solid-state IR $\nu_{CN}$ bands of $CNAr^{Clips2}$ (2132 $cm^{-1}$) and $CNAr^{DArF2}$ (2119 $cm^{-1}$) may also be compared with those of the alkyl-substituted isocyanides $CNAr^{Dipp2}$ and $CNAr^{Mes2}$. The latter exhibit solid-state $\nu_{CN}$ bands of 2124 $cm^{-1}$ and 2120 $cm^{-1}$, respectively. This series of IR data thereby demonstrate that substituent changes on flanking rings or the *para*-position of the *m*-terphenyl framework can have a measured effect on the $\nu_{CN}$ band of the uncoordinated, terminal isocyano unit. This observation is in contrast to previous IR and computational studies on *para*- and *ortho*- monosubstituted aryl isocyanides, which have argued that the energy of $\nu_{CN}$ bands is not appreciably influenced by substituent changes.[86,87]

**3. $\eta^6$-Arene Molybdenum Complexes Supported by $CNAr^{Clips2}$.** Relative to $CNAr^{Dipp2}$ and $CNAr^{Mes2}$, dichlorophenyl-substituted $CNAr^{Clips2}$ displays a lower initial propensity for flanking-ring binding upon reaction with molybdenum $\eta^6$-arene starting materials. Treatment of $Mo(\eta^6\text{-}C_{10}H_8)_2$ with 3.0 equiv of $CNAr^{Clips2}$ in *n*-pentane solution results in the formation of the $\eta^6$-naphthalene complex, $Mo(\eta^6\text{-}C_{10}H_8)(CNAr^{Clips2})_3$ ($\mathbf{3}^{Clips}$; Scheme 4; Figure 4a). This outcome contrasts with the reactivity of both $CNAr^{Dipp2}$ and $CNAr^{Mes2}$ toward $Mo(\eta^6\text{-}C_{10}H_8)_2$, where flanking-ring $\eta^6$-arene binding is rapid and the corresponding $\eta^6$-naphthalene-tris(isocyanide) complexes are not observed (i.e., $Mo(\eta^6\text{-}C_{10}H_8)(CNR)_3$; R = $Ar^{Dipp2}$ or $Ar^{Mes2}$). $\eta^6$-Binding of the 2,6-dichlorophenyl group in $CNAr^{Clips2}$ is also disfavored relative to the binding of benzene and fluorobenzene when these solvents are used in conjunction with the $Mo(\eta^6\text{-}C_{10}H_8)_2$ starting material. Thus, treatment of $Mo(\eta^6\text{-}C_{10}H_8)_2$ with 3.0 equiv of $CNAr^{Clips2}$ in either $C_6H_6$ or $C_6H_5F$ at room temperature results in the rapid formation of the $\eta^6$-arene complexes, $Mo(\eta^6\text{-}C_6H_6)(CNAr^{Clips2})_3$ ($\mathbf{4}^{Clips}$) and $Mo(\eta^6\text{-}C_6H_5F)(CNAr^{Clips2})_3$ ($\mathbf{5}^{Clips}$), respectively (Scheme 4; Figure 4b−c). The molecular structures of $Mo(\eta^6\text{-}C_{10}H_8)(CNAr^{Clips2})_3$ ($\mathbf{3}^{Clips}$), $Mo(\eta^6\text{-}C_6H_6)(CNAr^{Clips2})_3$ ($\mathbf{4}^{Clips}$), and $Mo(\eta^6\text{-}C_6H_5F)(CNAr^{Clips2})_3$ ($\mathbf{5}^{Clips}$) as determined by X-ray diffraction are shown in Figure 4. Each complex adopts the standard three-legged piano stool structural motif and exhibits a roughly $C_3$-symmetric orientation of $CNAr^{Clips2}$ ligands. The molybdenum centers in the benzene and fluorobenzene complexes $\mathbf{4}^{Clips}$ and $\mathbf{5}^{Clips}$ display symmetric coordination of the $\eta^6$-arene carbon atoms. In contrast, complex $\mathbf{3}^{Clips}$ displays an asymmetric $\eta^6$-arene interaction that is "slipped" away from the ring-junction carbon atoms of the naphthalene ligand. These so-called "flat-slipped" $\eta^6$-interactions are well documented and arise to maximize


dx.doi.org/10.1021/ic402130p | Inorg. Chem. 2013, 52, 13216−13229

**Scheme 3**

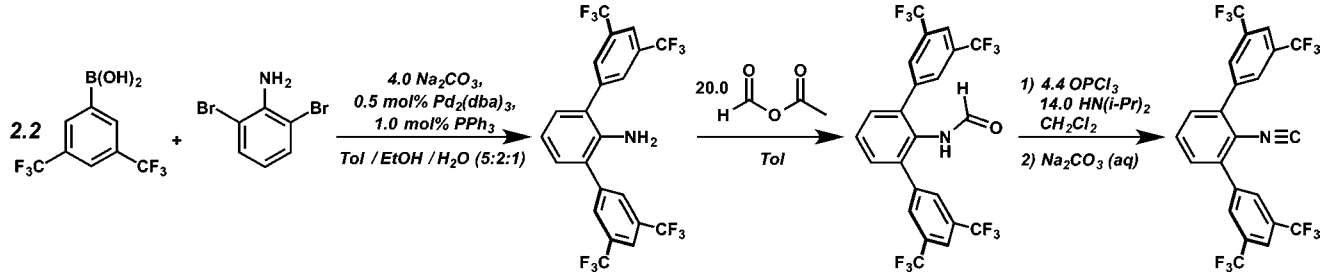


**Scheme 4**

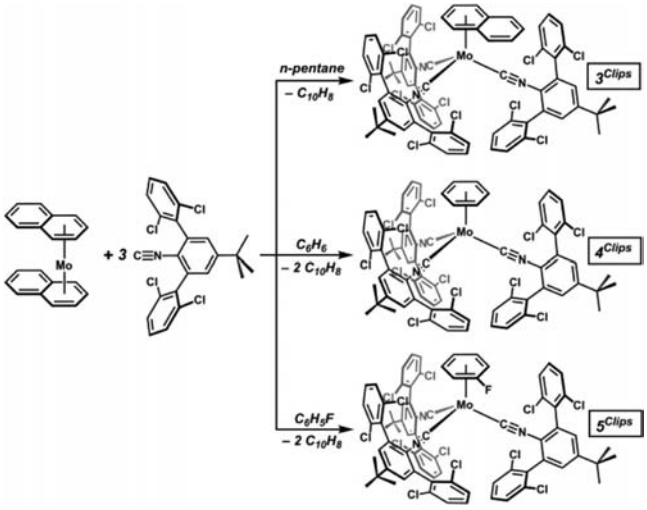


orbital overlap between the metal center and the highest occupied molecular orbital (HOMO) of naphthalene, which possesses a node at the ring-junction carbon atoms.[66,88]

Although an $\eta^6$-dichlorophenyl interaction does not form upon reaction of $CNAr^{Clips2}$ with $Mo(\eta^6\text{-}C_{10}H_8)_2$ at room temperature, its formation can be induced from thermolysis of the resultant products. Accordingly, heating *n*-pentane solutions of either $Mo(\eta^6\text{-}C_{10}H_8)(CNAr^{Clips2})_3$ ($\mathbf{3}^{Clips}$) or $Mo(\eta^6\text{-}C_6H_6)(CNAr^{Clips2})_3$ ($\mathbf{4}^{Clips}$) at 60 °C for 12 h results in arene loss and formation of the $\eta^6$-dichlorophenyl complex, $Mo(\eta^6\text{-}(2,6\text{-}Cl_2C_6H_3)\text{-}\kappa^1\text{-}C\text{-}CNAr^{Clips})(CNAr^{Clips2})_2$ ($\mathbf{1}^{Clips}$; Scheme 5). Structural characterization of $\mathbf{1}^{Clips}$ (Figure 5) revealed a geometrically constrained isocyanide ligand similar to those found in $\mathbf{1}^{Dipp}$ and $\mathbf{1}^{Mes}$ (Table 1). The $^{13}C\{^1H\}$ NMR chemical shift and $\nu_{CN}$ IR stretch of the bent $C_{iso}$ atom in $\mathbf{1}^{Clips}$ are $\delta$ = 275.6 ppm ($C_6D_6$) and 1680 $cm^{-1}$ ($C_6D_6$), respectively, which are also similar to the spectroscopic properties found for $\mathbf{1}^{Dipp}$ and $\mathbf{1}^{Mes}$ (Table 1). Furthermore, like its alkyl-substituted analogues, $\mathbf{1}^{Clips}$ is resistant toward further reaction at room temperature with coordinating solvents, such as acetonitrile and THF, as well as arene solvents such as benzene and toluene. Thus, although the 2,6-dichlorophenyl group of $CNAr^{Clips2}$ does not readily displace $\eta^6$-coordinated arenes, once bound, it is not readily displaced from the molybdenum center by more electron-releasing arenes.

While it can be isolated in pure form, it is important to note that the $\eta^6$-dichlorophenyl complex $\mathbf{1}^{Clips}$ is not formed exclusively upon thermolysis of $\mathbf{3}^{Clips}$ or $\mathbf{4}^{Clips}$. As shown in Scheme 5, these thermolysis reactions produce $\mathbf{1}^{Clips}$ along with the paramagnetic tetraisocyanide-dichloride complex $MoCl_2(CNAr^{Clips2})_4$ ($\mathbf{6}^{Clips}$) and the diphenanthridine **7**. Thermolysis of either $\mathbf{3}^{Clips}$ or $\mathbf{4}^{Clips}$ produce $\mathbf{1}^{Clips}$ and diphenanthridine **7** in roughly a 4:1 ratio as determined by $^1H$ NMR spectroscopy, and we presume that paramagnetic dichloride $\mathbf{6}^{Clips}$ is generated in roughly equimolar quantities to **7**.[89] Each compound can be isolated by successive washings in benzene, thereby enabling their full characterization by NMR spectroscopic and X-ray diffraction methods (Figures 6–7).

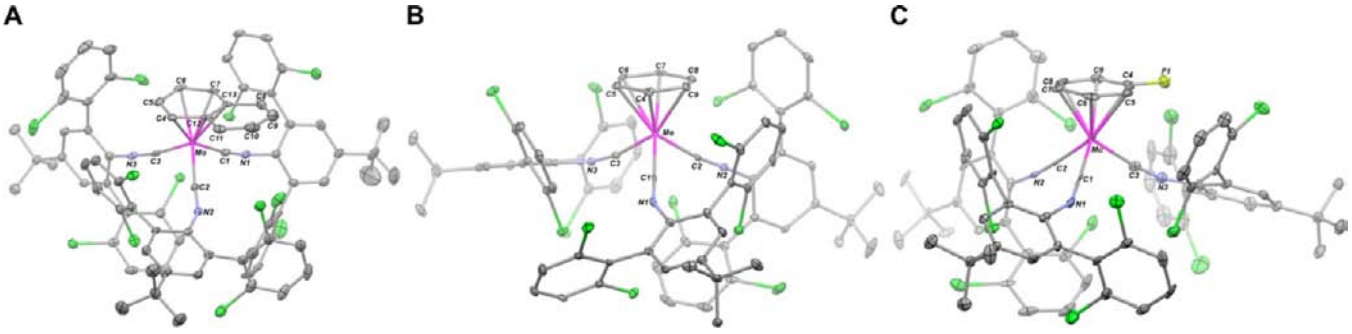


**Figure 4.** (A) Molecular structure of $Mo(\eta^6\text{-}C_{10}H_8)(CNAr^{Clips2})_3$ ($\mathbf{3}^{Clips}$). Selected bond distances (Å) and angles (deg): Mo1–C1 = 2.035(8); Mo1–C2 = 2.015(7); Mo1–C3 = 1.998(8); Mo1–C4 = 2.325(8); Mo1–C5 = 2.319(8); Mo1–C6 = 2.313(8); Mo1–C7 = 2.287(7); Mo1–C12 = 2.461(8); Mo1–C13 = 2.424(8); C1–Mo1–C2 = 95.3(2); C1–Mo1–C3 = 90.9(3); C2–Mo1–C3 = 95.7(3). (B) Molecular structure of $Mo(\eta^6\text{-}C_6H_6)(CNAr^{Clips2})_3$ ($\mathbf{4}^{Clips}$). Selected bond distances (Å) and angles (deg): Mo1–C1 = 2.020(4); Mo1–C2 = 2.013(4); Mo1–C3 = 1.995(4); Mo1–C4 = 2.322(4); Mo1–C5 = 2.358(4); Mo1–C6 = 2.310(4); Mo1–C7 = 2.326(4); Mo1–C8 = 2.302(4); Mo1–C9 = 2.352(4); C1–Mo1–C2 = 92.83(14); C1–Mo1–C3 = 96.17(14); C2–Mo1–C3 = 90.75(15). (C) Molecular structure of $Mo(\eta^6\text{-}C_6H_5F)(CNAr^{Clips2})_3$ ($\mathbf{5}^{Clips}$). Selected bond distances (Å) and angles (deg): Mo1–C1 = 2.016(8); Mo1–C2 = 2.029(7); Mo1–C3 = 2.011(8); Mo1–C4 = 2.316(9); Mo1–C5 = 2.348(8); Mo1–C6 = 2.297(7); Mo1–C7 = 2.346(7); Mo1–C8 = 2.277(7); Mo1–C9 = 2.322(8); C1–Mo1–C2 = 89.8(3); C1–Mo1–C3 = 96.5(3); C2–Mo1–C3 = 89.1(3).


dx.doi.org/10.1021/ic402130p | *Inorg. Chem.* 2013, 52, 13216–13229

Scheme 5

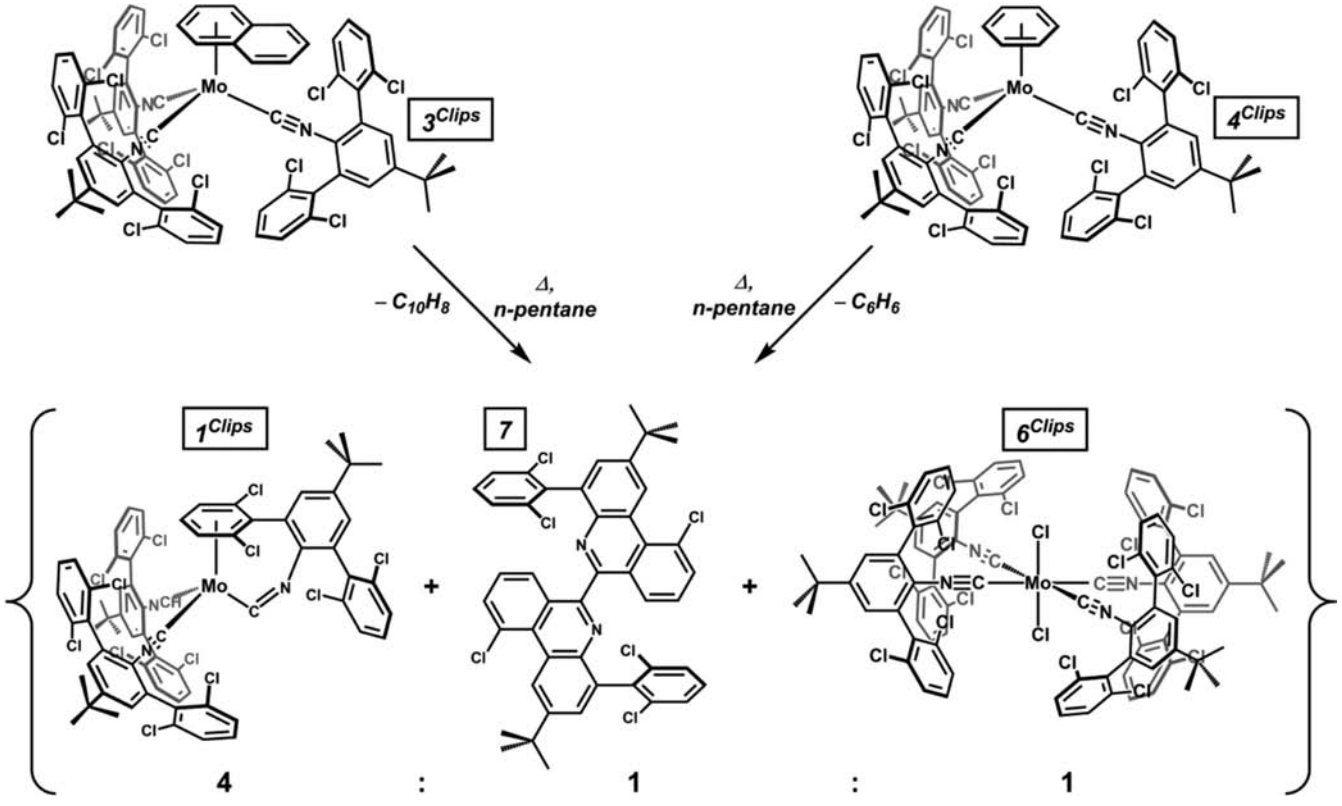


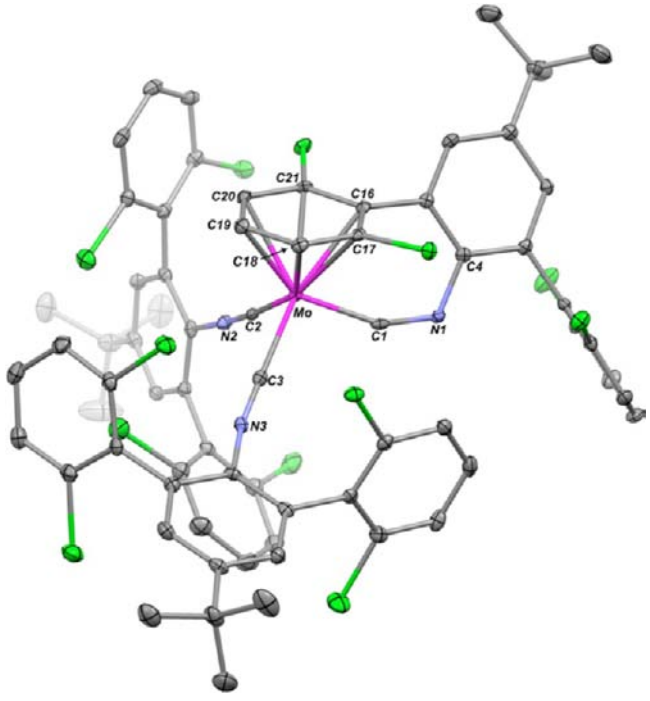


**Figure 5.** Molecular structure Mo($\eta^6$-(2,6-$Cl_2C_6H_3$)-$\kappa^1$-C-$CNAr^{Clips}$)-($CNAr^{Clips2}$)$_2$ (**1**$^{Clips}$). Selected bond distances (Å) and angles (deg): Mo1−C1 = 1.928(3); Mo1−C2 = 2.036(3); Mo1−C3 = 2.051(3); C1−N1 = 1.235(4); N1−C4 = 1.408(4); Mo1−C16 = 2.316(3); Mo1−C17 = 2.323(3); Mo1−C18 = 2.333(3); Mo1−C19 = 2.334(3); Mo1−C20 = 2.330(3); Mo1−C21 = 2.314(3); C1−Mo1−C2 = 96.55(11); C1−Mo1−C3 = 98.50(11); C2−Mo1−C3 = 89.18(11); Mo1−C1−N1 = 153.5(2); C1−N1−C4 = 120.1(2).

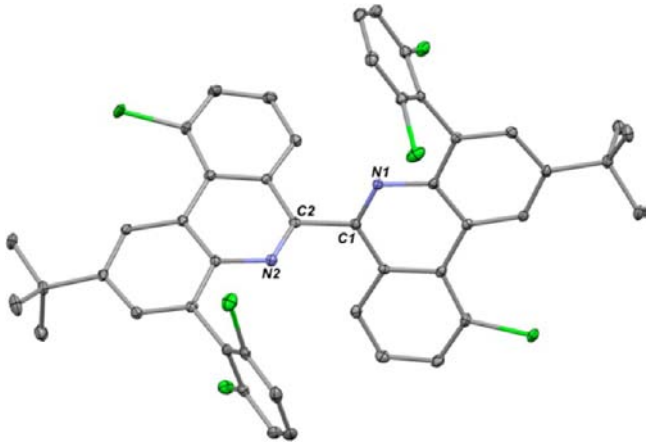


**Figure 6.** Molecular structure of 2,2′-di-*tert*-butyl-10,10′-dichloro-4,4′-bis(Clips)-6,6′-biphenanthridine (**7**). Selected bond distances (Å) and angles (deg): C1−C2 = 1.500(3); C2−N2 = 1.303(3); C1−N1 = 1.303(3).

The formation of diphenanthridine **7** can be rationalized as a product resulting from chlorine-atom abstraction, phenyl-radical addition to an isocyanide unit, and bimolecular coupling of two cyclized, $Ar^{Clips}$-based phenanthridine radicals. The initiation step in this sequence is likely chlorine-atom transfer from a $CNAr^{Clips2}$ ligand to a low-valent molybdenum center, which then enables the formation of $MoCl_2(CNAr^{Clips2})_4$ (**6**$^{Clips}$). Contrastingly however, heating pure **1**$^{Clips}$ at 90 °C in cyclohexane-$d_{12}$ produces only trace quantities of **6**$^{Clips}$ and **7** after a 24 h period. This observation suggests that independent arene-displacement and chlorine-atom-abstraction pathways are available at elevated temperatures to the $\eta^6$-naphthalene and $\eta^6$-


dx.doi.org/10.1021/ic402130p | *Inorg. Chem.* 2013, 52, 13216−13229

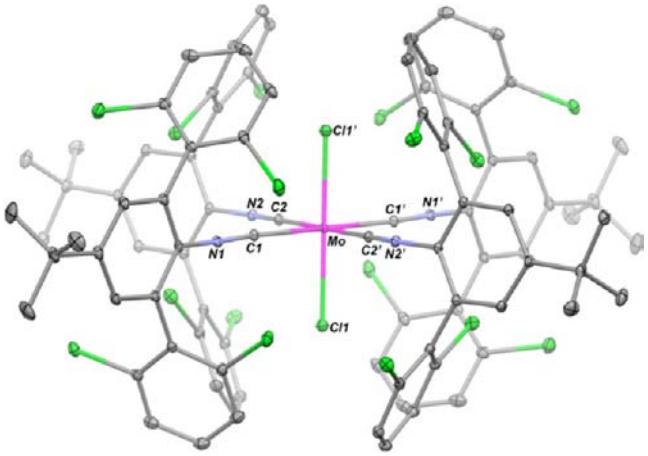


**Figure 7.** Molecular structure of $MoCl_2(CNAr^{Clips2})_4$ ($\mathbf{6}^{Clips}$). Selected bond distances (Å) and angles (deg): Mo1−C1 = 2.1117(9); Mo1−C2 = 2.1129(9); Mo1−Cl1 = 2.4058(3); C1−Mo1−C2 = 88.99(3); C1−Mo1−Cl1 = 87.57(3); C2−Mo1−Cl1 = 89.79(3).

benzene complexes $\mathbf{3}^{Clips}$ or $\mathbf{4}^{Clips}$, respectively, whereas $\eta^6$-binding of a $CNAr^{Clips2}$ ligand by molybdenum evidently inhibits chlorine-atom abstraction.

**4. $\eta^6$-Arene Molybdenum Complexes Supported by $CNAr^{DArF2}$.** The coordination properties of trifluoromethyl-substituted $CNAr^{DArF2}$ toward zerovalent molybdenum centers mirror those of $CNAr^{Clips2}$, but its resultant complexes display significantly different behavior. In analogy to the $CNAr^{Clips2}$ system, treatment of $Mo(\eta^6\text{-}C_{10}H_8)_2$ with 3 equiv of $CNAr^{DArF2}$ in *n*-pentane generates the isolable $\eta^6$-naphthalene tris-isocyanide complex, $Mo(\eta^6\text{-}C_{10}H_8)(CNAr^{DArF2})_3$ ($\mathbf{3}^{DArF}$; Scheme 6). The latter was characterized by X-ray diffraction

**Scheme 6**

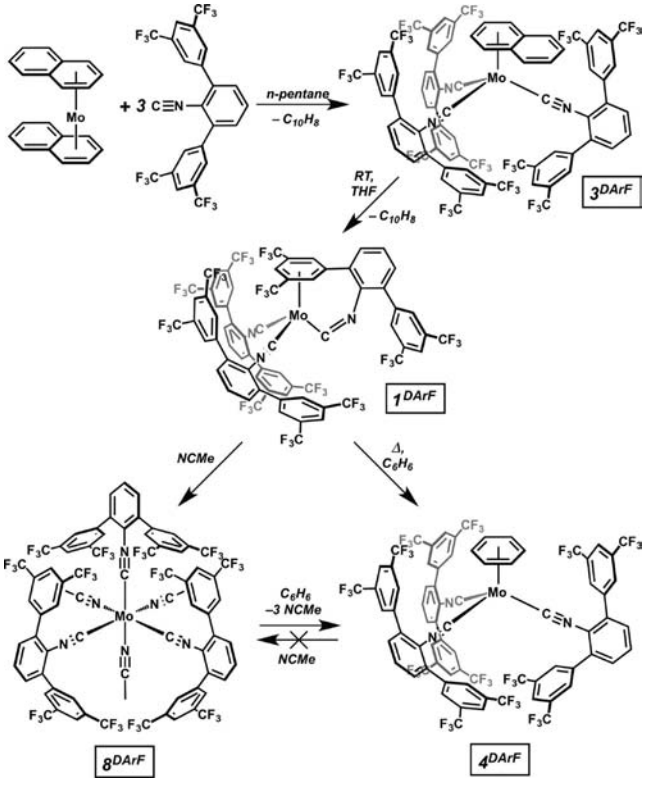


(Figure 8) and possesses structural features largely similar to $Mo(\eta^6\text{-}C_{10}H_8)(CNAr^{Clips2})_3$ ($\mathbf{3}^{Clips}$), including the "flat-slipped"

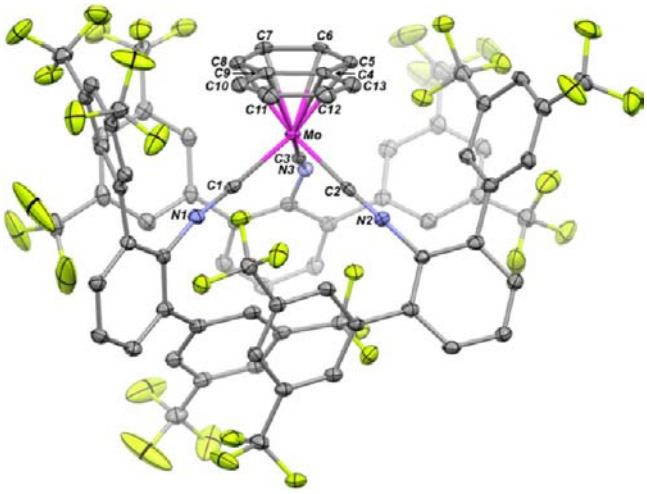


**Figure 8.** Molecular structure of $Mo(\eta^6\text{-}C_{10}H_8)(CNAr^{DArF2})_3$ ($\mathbf{3}^{DArF}$). Selected bond distances (Å) and angles (deg): Mo1−C1 = 2.012(4); Mo1−C2 = 2.011(4); Mo1−C3 = 1.961(5); Mo1−C4 = 2.441(4); Mo1−C5 = 2.343(4); Mo1−C6 = 2.331(4); Mo1−C7 = 2.325(4); Mo1−C8 = 2.319(4); Mo1−C9 = 2.440(4); C1−Mo1−C2 = 91.29(15); C1−Mo1−C3 = 90.00(15); C2−Mo1−C3 = 90.37(16).

$\eta^6$-interaction of the coordinated naphthalene ring. However, the solid-state structure of $Mo(\eta^6\text{-}C_{10}H_8)(CNAr^{DArF2})_3$ ($\mathbf{3}^{DArF}$) reveals, qualitatively, that the $CNAr^{DArF}$ ligand imparts a significantly higher degree of steric crowding around the central metal center than is found in similar $CNAr^{Mes2}$-, $CNAr^{Dipp2}$-, or $CNAr^{Clips2}$-ligated systems.

Whereas $Mo(\eta^6\text{-}C_{10}H_8)(CNAr^{DArF2})_3$ ($\mathbf{3}^{DArF}$) is isolable, it is found to cleanly form the $\eta^6$-bis-(trifluoromethyl)phenyl complex $Mo(\eta^6\text{-}(3,5\text{-}(CF_3)_2C_6H_3)\text{-}\kappa^1\text{-}C\text{-}CNAr^{DArF})(CNAr^{DArF2})_2$ ($\mathbf{1}^{DArF}$; Scheme 6) at room temperature over the course of 12 h. As monitored by $^1$H NMR spectroscopy, an equivalent of naphthalene is lost upon $\eta^6$-bis-(trifluoromethyl)-phenyl group binding. This behavior is clearly different than that of $CNAr^{Clips2}$-ligated $Mo(\eta^6\text{-}C_{10}H_8)(CNAr^{Clips2})_3$ ($\mathbf{3}^{Clips}$), which requires elevated temperatures to furnish a $\eta^6$-dichlorophenyl interaction. While 3,5-bis(trifluoromethyl)-phenyl groups display a low propensity for $\eta^6$-arene binding,[84,85] we tentatively suggest that steric pressures[90] within the $\eta^6$-naphthalene complex $Mo(\eta^6\text{-}C_{10}H_8)(CNAr^{DArF2})_3$ ($\mathbf{3}^{DArF}$) may provide for a low-energy pathway to flanking-ring $\eta^6$-binding of $CNAr^{DArF2}$ and naphthalene release. Alternatively, the peripheral $CF_3$ groups of the $CNAr^{DArF2}$ framework may provide a coordinatively assisted pathway to 3,5-bis-(trifluoromethyl)phenyl group binding,[66] especially if $\eta^6$-naphthalene ring-slippage is facile within $Mo(\eta^6\text{-}C_{10}H_8)$-$(CNAr^{DArF2})_3$ ($\mathbf{3}^{DArF}$). However, evidence for such a process has not been obtained for $Mo(\eta^6\text{-}C_{10}H_8)(CNAr^{DArF2})_3$ ($\mathbf{3}^{DArF}$) to date.

Crystallographic characterization of $Mo(\eta^6\text{-}(3,5\text{-}(CF_3)_2C_6H_3)\text{-}\kappa^1\text{-}C\text{-}CNAr^{DArF})(CNAr^{DArF2})_2$ ($\mathbf{1}^{DArF}$; Figure 9) revealed structural features similar to its $CNAr^{Mes2}$, $CNAr^{Dipp2}$, and $CNAr^{Clips2}$ analogues (Table 1), along with added steric congestion from the 3,5-$CF_3$ groups. The bent $C_{iso}$ carbon in $\mathbf{1}^{DArF}$ also displays spectroscopic features consistent with the other geometrically constrained isocyanide ligands presented in this study (Table 1).


dx.doi.org/10.1021/ic402130p | *Inorg. Chem.* 2013, 52, 13216−13229

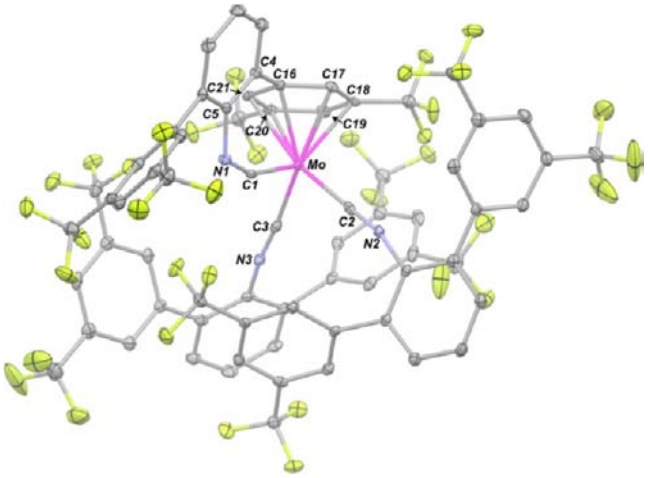


**Figure 9.** Molecular structure of Mo($\eta^6$-(3,5-$(CF_3)_2C_6H_3$)-$\kappa^1$-*C*-$CNAr^{DArF}$)$(CNAr^{DArF2})_2$ ($\mathbf{1}^{DArF}$). Selected bond distances (Å) and angles (deg): Mo1−C1 = 1.947(3); Mo1−C2 = 2.048(3); Mo1−C3 = 2.037(3); C1−N1 = 1.229(4); N1−C5 = 1.410(4); Mo1−C16 = 2.307(3); Mo1−C17 = 2.340(3); Mo1−C18 = 2.316(3); Mo1−C19 = 2.334(3); Mo1−C20 = 2.292(3); Mo1−C21 = 2.300(3); C1−Mo1−C2 = 96.19(12); C1−Mo1−C3 = 90.74(12); C2−Mo1−C3 = 90.28(12); Mo1−C1−N1 = 153.9(2); C1−N1−C5 = 120.8(3).

Unlike the flanking-ring $\eta^6$-arene interactions in complexes $\mathbf{1}^{Dipp}$, $\mathbf{1}^{Mes}$, and $\mathbf{1}^{Clips}$, the coordinated bis(trifluoromethyl)-phenyl group in $\mathbf{1}^{DArF}$ can be released from the metal center upon addition of substrates. As shown in Scheme 6, dissolution of Mo($\eta^6$-(3,5-$(CF_3)_2C_6H_3$)-$\kappa^1$-*C*-$CNAr^{DArF}$)$(CNAr^{DArF2})_2$ ($\mathbf{1}^{DArF}$) in $C_6H_6$ solution followed by heating at 100 °C for 6 days provides the $\eta^6$-benzene complex ($\eta^6$-$C_6H_6$)Mo-$(CNAr^{DArF})_3$ ($\mathbf{4}^{DArF}$; Figure 10). Although displacement of the coordinated bis(trifluoromethyl)phenyl group in $\mathbf{1}^{DArF}$ by benzene is sluggish, it is in direct contrast to the behavior demonstrated by $\mathbf{1}^{Dipp}$, $\mathbf{1}^{Mes}$, and $\mathbf{1}^{Clips}$ under similar conditions. This reactivity profile therefore demonstrates that the bis-(trifluoromethyl)phenyl group of the $CNAr^{DArF2}$ ligand can be used to effectively mask the zerovalent molybdenum tris-isocyanide fragment [Mo$(CNAr^{DArF2})_3$] in the form of the tethered $\eta^6$-arene complex $\mathbf{1}^{DArF}$. Furthermore, it is apparent that flanking-ring $\eta^6$-arene interactions to molybdenum from $CNAr^{Dipp2}$, $CNAr^{Mes2}$, and $CNAr^{Clips2}$ do not function similarly in this regard.

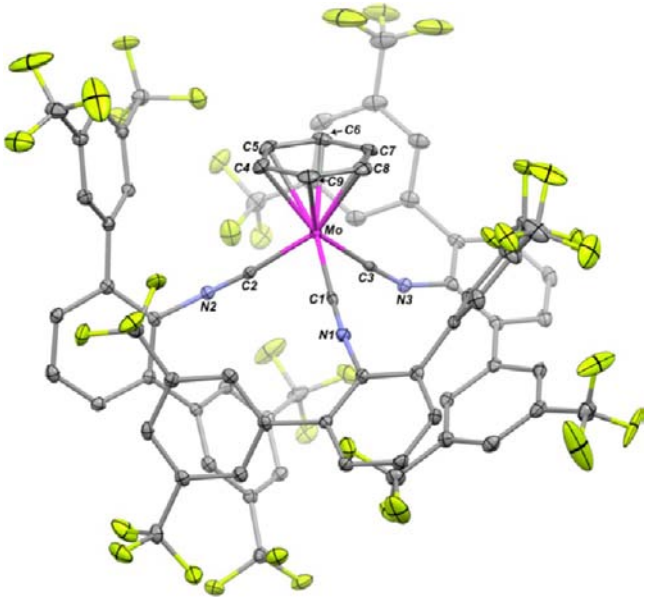


**Figure 10.** Molecular structure of Mo($\eta^6$-$C_6H_6$)$(CNAr^{DArF2})_3$ ($\mathbf{4}^{DArF}$). Selected bond distances (Å) and angles (deg): Mo1−C1 = 1.989(3); Mo1−C2 = 1.991(3); Mo1−C3 = 1.998(3); Mo1−C4 = 2.297(17); Mo1−C5 = 2.289(16); Mo1−C6 = 2.289(16); Mo1−C7 = 2.299(17); Mo1−C8 = 2.307(18); Mo1−C9 = 2.306(18); C1−Mo1−C2 = 91.00(11); C1−Mo1−C3 = 87.55(11); C2−Mo1−C3 = 92.72(11).

While benzene reacts with $\mathbf{1}^{DArF}$ at elevated temperatures, it is far more notable that $\eta^6$-bis(trifluoromethyl)phenyl group displacement is significantly more facile upon addition of stronger Lewis bases. Thus, dissolution of $\mathbf{1}^{DArF}$ in acetonitrile solution at room temperature rapidly results in a color change from orange to purple, concomitant with the formation of *fac*-Mo$(NCMe)_3(CNAr^{DArF2})_3$ ($\mathbf{8}^{DArF}$). Structural characterization on purple single crystals of $\mathbf{8}^{DArF}$ obtained from the reaction mixture confirmed that three acetonitrile molecules combine to displace the $\eta^6$-bound 3,5-$(CF_3)_2C_6H_3$ group in $\mathbf{1}^{DArF}$, resulting in three terminally bound $CNAr^{DArF}$ ligands (Figure 11). $^1$H

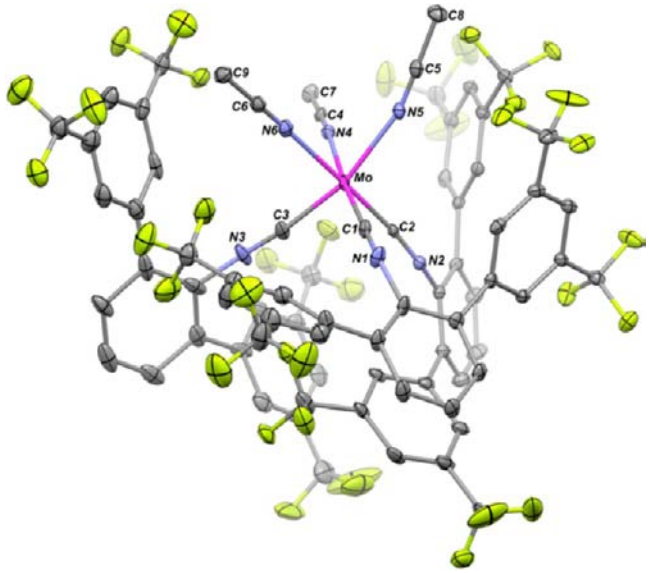


**Figure 11.** Molecular structure of *fac*-Mo$(NCMe)_3(CNAr^{DArF2})_3$ ($\mathbf{8}^{DArF}$). Selected bond distances (Å) and angles (deg): Mo1−C1 = 1.929(11); Mo1−C2 = 1.961(5); Mo1−C3 = 1.939(12); Mo1−N4 = 2.231(5); Mo1−N5 = 2.242(5); Mo1−N6 = 2.233(5); C1−Mo1−C2 = 86.8(4); C1−Mo1−C3 = 95.5(4); C1−Mo1−N4 = 173.9(2); C1−Mo1−N5 = 94.1(2); C1−Mo1−N6 = 95.1(18); C2−Mo1−C3 = 89.8(3); C2−Mo1−N4 = 88.69(19); C2−Mo1−N5 = 103.20(18); C2−Mo1−N6 = 177.44(19); C3−Mo1−N4 = 88.6(4); C3−Mo1−N5 = 164.3(3); C3−Mo1−N6 = 88.3(3); N4−Mo1−N5 = 82.93(16); N4−Mo1−N6 = 89.54(17); N5−Mo1−N6 = 78.42(17).

NMR analysis of the $\mathbf{1}^{DArF}$ to $\mathbf{8}^{DArF}$ conversion in acetonitrile-$d_3$ indicated that the displacement of $\eta^6$-bound 3,5-$(CF_3)_2C_6H_3$ group is complete upon mixing and that it does not reversibly coordinate over 3 days when excess acetonitrile is present. However, addition of an excess of benzene to a acetonitrile-$d_3$ solution of $\mathbf{8}^{DArF}$, or dissolution of single crystalline $\mathbf{8}^{DArF}$ in benzene, rapidly generates the $\eta^6$-benzene complex ($\eta^6$-$C_6H_6$)Mo$(CNAr^{DArF2})_3$ ($\mathbf{4}^{DArF}$, Scheme 6). Excess acetonitrile does not displace the $\eta^6$-benzene ligand from $\mathbf{4}^{DArF}$, which further highlights the lability of the $\eta^6$-(3,5-$(CF_3)_2C_6H_3$) group


dx.doi.org/10.1021/ic402130p | *Inorg. Chem.* 2013, 52, 13216−13229

present in $\mathbf{1}^{DArF}$. We are currently probing the scope of coodinative displacement of the $\eta^6$-(3,5-$(CF_3)_2C_6H_3$) group of $\mathbf{1}^{DArF}$ with additional substrates to ascertain whether this flanking-ring-bound *m*-terphenyl isocyanide complex serves reliably as a functional equivalent of [$Mo(CNAr^{DArF2})_3$].

**5. Electronic Comparison of Chloro-, Trifluoromethyl-, and Alkyl-Substituted *m*-Terphenyl Isocyanide Ligands.** In addition to probing $\eta^6$-arene binding by alkyl-, chloro-, and trifluoromethyl-substituted *m*-terphenyl isocyanides, we have also assessed the relative electronic influences these ligands impart on metal centers in their terminal-isocyanide binding mode. Given that their electron-withdrawing substituents are fairly distal to, and not $\pi$-conjugated with, the isocyanide unit, we were particularly interested in whether $CNAr^{Clips2}$ and $CNAr^{DArF2}$ displayed increased $\pi$-acceptor properties relative to isocyanides based on more traditional *m*-terphenyl frameworks. As a point of reference, it has previously been shown that the $\pi$-acceptor properties of coordinated aryl isocyanides can be modulated most broadly by the identity of a substituent *para* to the isocyanide unit.[87,91,92] In general, the $\pi$-acceptor ability of *para*-substituted aryl isocyanides increase in the order MeO < Me < H < F < Cl < $NO_2$.[87] Modulation of *meta*-substituents has also been shown to affect the $\pi$-acceptor properties of aryl isocyanides, but to a lesser extent than found for similar substituent variation in the *para*-position. The electronic effects of *ortho*-substitution have not been studied systematically. However, computational work by Cooper has suggested that *ortho* substitutents have a more pronounced effect on the $\sigma$-donating ability of aryl isocyanides, rather than on their $\pi$-acceptor properties.[87]

To determine the electronic influences of $CNAr^{Clips2}$ and $CNAr^{DArF2}$, we targeted *fac*- and *mer*-tricarbonyl tris-isocyanide complexes of molybdenum (i.e., $Mo(CO)_3(CNAr^R)_3$). Such targets allow for direct IR spectroscopic comparison to the previously reported $CNAr^{Mes2}$ derivatives *fac*-$Mo(CO)_3(CNAr^{Mes2})_3$ (*fac*-$\mathbf{9}^{Mes}$) and *mer*-$Mo(CO)_3(CNAr^{Mes2})_3$ (*mer*-$\mathbf{9}^{Mes}$).[40] Schemes 7 and 8 outline ligand-substitution and/

**Scheme 7**

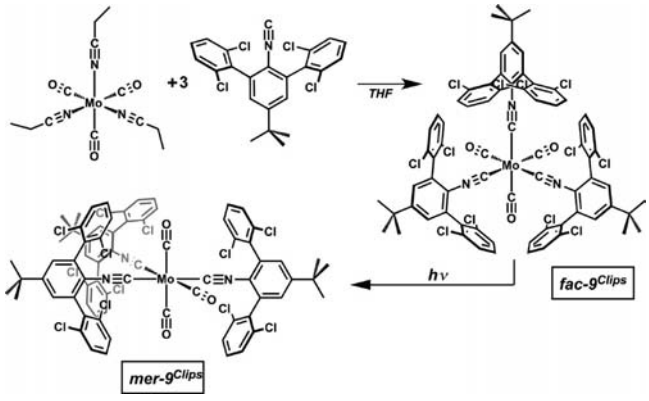


or photochemical routes to the $CNAr^{Clips2}$ and $CNAr^{DArF2}$ complexes *fac*-$Mo(CO)_3(CNAr^{Clips2})_3$ (*fac*-$\mathbf{9}^{Clips}$), *mer*-$Mo(CO)_3(CNAr^{Clips2})_3$ (*mer*-$\mathbf{9}^{Clips}$) and *mer*-$Mo(CO)_3(CNAr^{DArF2})_3$ (*mer*-$\mathbf{9}^{DArF}$). Each complex has been crystallographically characterized (Figures 12−14) and exhibits NMR and IR spectroscopic features in solution consistent with its solid-state structure. To date, all attempts to prepare the *fac*-derivative of $Mo(CO)_3(CNAr^{DArF2})_3$ by thermal or photochemical methods have instead led to the isolation of its *mer*

**Scheme 8**

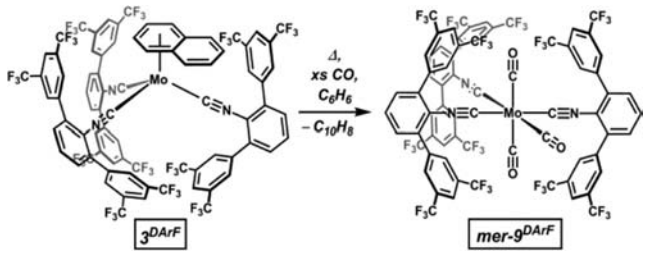


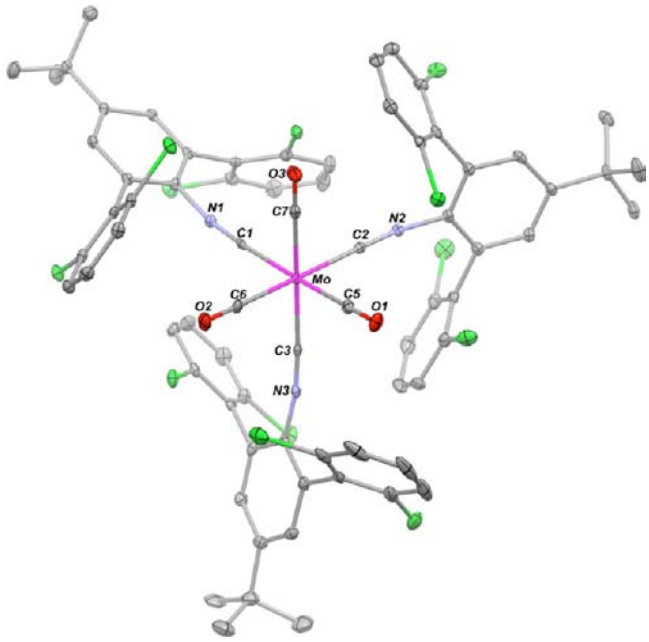


**Figure 12.** Molecular structure of *fac*-$Mo(CO)_3(CNAr^{Clips2})_3$ (*fac*-$\mathbf{9}^{Clips}$). Selected bond distances (Å) and angles (deg): Mo1−C1 = 2.103(3); Mo1−C2 = 2.101(3); Mo1−C3 = 2.106(3); Mo1−C5 = 2.019(3); Mo1−C6 = 2.035(3); Mo1−C7 = 2.009(3); C1−Mo1−C2 = 93.12(11); C1−Mo1−C3 = 94.13(11); C1−Mo1−C5 = 175.79(11); C1−Mo1−C6 = 89.30(11); C1−Mo1−C7 = 87.34(11); C2−Mo1−C3 = 93.70(11); C2−Mo1−C5 = 88.15(11); C2−Mo1−C6 = 176.59(11); C2−Mo1−C7 = 88.15(11); C3−Mo1−C5 = 89.79(11); C3−Mo1−C6 = 88.52(12); C3−Mo1−C7 = 177.57(12); C5−Mo1−C6 = 89.27(12); C5−Mo1−C7 = 89.27(12); C6−Mo1−C7 = 89.55(12).

isomer. While steric pressures between three $CNAr^{DArF2}$ ligands may destabilize the *fac*-isomer of $Mo(CO)_3(CNAr^{DArF2})_3$,[40] it is important to note that the perfluorinated-isocyanide tungsten tricarbonyl complexes $W(CO)_3(CNCF_3)_3$ and $W(CO)_3(CNC_6F_5)_3$ prepared by Lentz exhibit a pronounced electronic preference for their *mer*-isomers.[93−95] Although it is presently unclear, a similar electronic preference for the *mer*-$Mo(CO)_3(CNR)_3$ isomer may potentially be displayed by the $Ar^{DArF}$ framework. It is also noteworthy that our attempts to prepare either *fac*- or *mer*-$Mo(CO)_3(CNAr^{Dipp2})_3$ have been unsuccessful and have resulted typically in the formation of the bis-isocyanide tetracarbonyl complex $Mo(CO)_4(CNAr^{Dipp2})_2$.[43] Again, we believe that is observation is the result of steric pressures associated with the encumbering $CNAr^{Dipp2}$ framework. Accordingly, in this study, we limit the electronic comparison of $CNAr^{Clips2}$ and $CNAr^{DArF2}$ to the dimesityl derivative $CNAr^{Mes2}$.


dx.doi.org/10.1021/ic402130p | Inorg. Chem. 2013, 52, 13216−13229

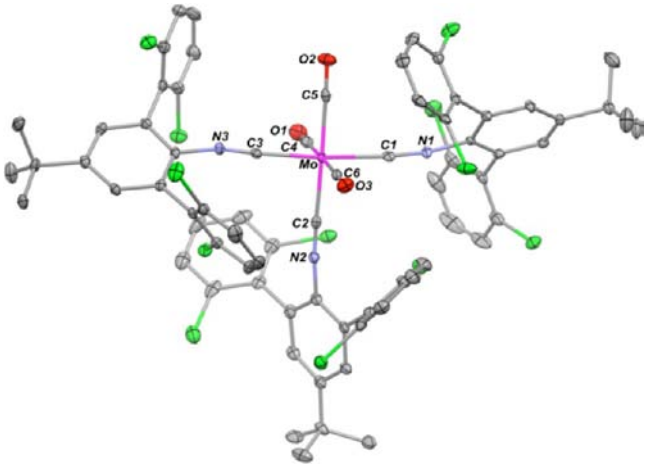


**Figure 13.** Molecular structure of *mer*-Mo(CO)$_3$(CNAr$^{Clips2}$)$_3$ (*mer*-**9**$^{Clips}$). Selected bond distances (Å) and angles (deg): Mo1−C1 = 2.077(5); Mo1−C2 = 2.119(5); Mo1−C3 = 2.070(5); Mo1−C4 = 2.044(6); Mo1−C5 = 2.015(5); Mo1−C6 = 2.045(5); C1−Mo1−C2 = 92.88(17); C1−Mo1−C3 = 173.65(18); C1−Mo1−C4 = 91.59(19); C1−Mo1−C5 = 87.50(19); C1−Mo1−C6 = 88.30(19); C2−Mo1−C3 = 92.87(18); C2−Mo1−C4 = 89.57(19); C2−Mo1−C5 = 177.1(2); C2−Mo1−C6 = 88.92(19); C3−Mo1−C4 = 91.16(19); C3−Mo1−C5 = 86.90(18); C3−Mo1−C6 = 89.10(19); C4−Mo1−C5 = 87.55(19); C4−Mo1−C6 = 178.5(2); C5−Mo1−C6 = 93.96(19).

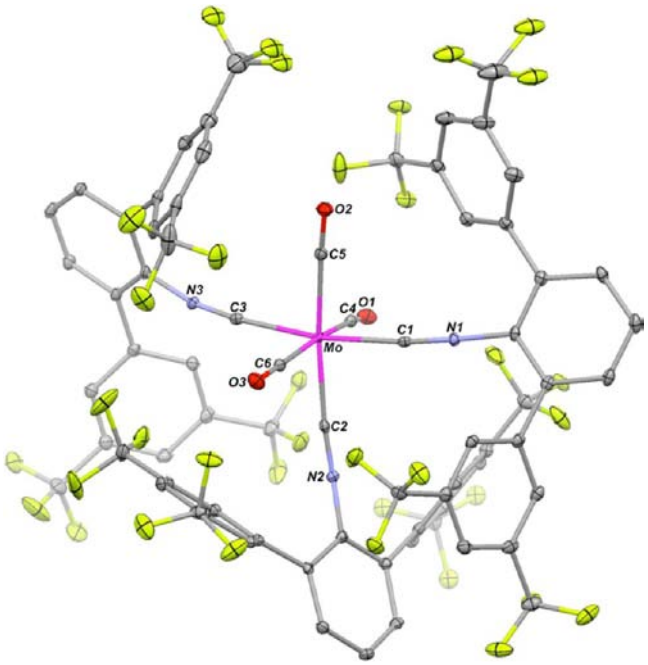


**Figure 14.** Molecular structure of *mer*-Mo(CO)$_3$(CNAr$^{DArF2}$)$_3$ (*mer*-**9**$^{DArF}$). Selected bond distances (Å) and angles (deg): Mo1−C1 = 2.067(3); Mo1−C2 = 2.083(4); Mo1−C3 = 2.070(4); Mo1−C4 = 2.044(5); Mo1−C5 = 2.035(4); Mo1−C6 = 2.050(4); C1−Mo1−C2 = 88.46(13); C1−Mo1−C3 = 169.89(13); C1−Mo1−C4 = 88.08(13); C1−Mo1−C5 = 84.14(13); C1−Mo1−C6 = 96.70(13); C2−Mo1−C3 = 99.06(13); C2−Mo1−C4 = 85.63(13); C2−Mo1−C5 = 170.03(13); C2−Mo1−C6 = 86.72(13); C3−Mo1−C4 = 85.78(13); C3−Mo1−C5 = 88.91(14); C3−Mo1−C6 = 90.51(13); C4−Mo1−C5 = 99.15(14); C4−Mo1−C6 = 170.86(14); C5−Mo1−C6 = 89.11(14).

Table 2 lists the $\nu_{CO}$ bands for complexes **9**$^{R}$ determined in $C_6D_6$ solution. For the *fac* partners *fac*-**9**$^{Mes}$ and *fac*-**9**$^{Clips}$, it is evident that CNAr$^{Clips2}$ and CNAr$^{Mes2}$ exert a very similar electronic influence on the molybdenum center. Whereas the flanking 2,6-dichlorphenyl groups of CNAr$^{Clips2}$ may be expected to slightly increase the $\pi$-acidity of the isocyano group, the *para tert*-butyl substituent may act to oppose this increase.[96] Comparison of the IR data for *mer*-**9**$^{Mes}$, *mer*-**9**$^{Clips}$, and *mer*-**9**$^{DArF}$ is less straightforward because of the fact that both *mer*-**9**$^{Clips}$ and *mer*-**9**$^{DArF}$ give rise to only a single $\nu_{CO}$ band, rather than three as expected for a $C_{2v}$-symmetric geometry (see the Supporting Infromation).[97] However, relative to *mer*-**9**$^{Mes}$ and *mer*-**9**$^{Clips}$, it is clear that *mer*-**9**$^{DArF}$ gives rise to a significantly blue-shifted $\nu_{CO}$ band, thereby indicating that the flanking 3,5-bis(trifluoromethyl)phenyl groups of CNAr$^{DArF}$ can indeed increase the $\pi$-acceptor properties of the isocyano group. Most importantly, this finding suggests that isocyanide ligands can be prepared that offer a large degree of steric encumbrance, while providing $\pi$-acceptor properties that begin to match that of CO. We believe this ligand design strategy will prove useful for the generation of low-coordinate isocyanide complexes that more accurately mimic the functional and spectroscopic behavior of the unsaturated binary metal carbonyls.[98]

**Table 2. Solution ($C_6D_6$) $\nu_{CN}$ and $\nu_{CO}$ Stretching Frequencies for Complexes 9$^{R}$**

| complex | $\nu_{CN}$ (cm$^{-1}$) | $\nu_{CO}$ (cm$^{-1}$) |
|---|---|---|
| *fac*-Mo(CO)$_3$(CNAr$^{Mes2}$)$_3$ (*fac*-**9**$^{Mes}$)[a] | 2046 (s) | 1942(s) |
| | 2000 (m) | 1910(s) |
| *fac*-Mo(CO)$_3$(CNAr$^{Clips2}$)$_3$ (*fac*-**9**$^{Clips}$) | 2042(s) | 1943(s) |
| | 2023(m sh) | 1909(vs) |
| *mer*-Mo(CO)$_3$(CNAr$^{Mes2}$)$_3$ (*mer*-**9**$^{Mes}$)[a] | 2046(m) | 1926(vs) |
| | 2024(s) | 1902(m) |
| | 1993(s) | |
| *mer*-Mo(CO)$_3$(CNAr$^{Clips2}$)$_3$ (*mer*-**9**$^{Clips}$) | 2038(m sh) | 1917(vs) |
| | 2010(s) | |
| | 1979(w sh) | |
| *mer*-Mo(CO)$_3$(CNAr$^{DArF2}$)$_3$ (*mer*-**9**$^{DArF}$) | 2040(m sh) | 1941(vs) |
| | 2006(s) | |
| | 1979(m sh) | |

[a]Data from reference 40.

## EXPERIMENTAL SECTION

**General Considerations.** All manipulations were carried out under an atmosphere of dry dinitrogen using standard Schlenk and glovebox techniques. Solvents were dried and deoxygenated according to standard procedures.[99] Unless otherwise stated, reagent-grade starting materials were purchased from commercial sources and either used as received or purified by standard procedures.[100] The *m*-terphenyl derivatives CNAr$^{Mes2}$, CNAr$^{Dipp2}$ and 2,6-(2,6-Cl$_2$C$_6$H$_3$)$_2$C$_6$H$_3$I were prepared according to literature procedures.[39,40,70b] *p*-Tolylsulfonyl azide (TosN$_3$) was prepared as described previously.[101] Benzene-$d_6$ and cyclohexane-$d_{12}$ (Cambridge Isotope Laboratories) were degassed and stored over 4 Å molecular sieves under N$_2$ for 2 d prior to use. Chloroform-*d* (Cambridge Isotope Laboratories) was vacuum distilled from NaH and then stored over 3 and 4 Å molecular sieves under N$_2$ for 2 d prior to use. Celite 405 (Fisher Scientific) was dried under vacuum (24 h) at a temperature above 250 °C and stored in the glovebox prior to use. Solution $^1$H, $^{13}$C{$^1$H} and $^{19}$F spectra were recorded on Varian Mercury 300 and 400 spectrometers, a Varian X-Sens500 spectrometer, or a JEOL ECA-500 spectrometer. $^1$H and $^{13}$C{$^1$H} chemical shifts are reported in


dx.doi.org/10.1021/ic402130p | Inorg. Chem. 2013, 52, 13216−13229

ppm relative to $SiMe_4$ ($^1H$ and $^{13}C$ $\delta$ = 0.0 ppm) with reference to residual solvent resonances of 7.16 ppm ($^1H$) and 128.06 ppm ($^{13}C$) for benzene-$d_6$, 1.38 ppm ($^1H$) and 26.43 ppm ($^{13}C$) for cyclohexane-$d_{12}$ and 7.26 ppm ($^1H$) and 77.23 ppm ($^{13}C$) for chloroform-$d$. $^{19}F$ NMR chemical shifts were referenced internally via capillary to neat trifluoroacetic acid $F_3CC(O)OH$ ($\delta$ = −78.5 ppm vs $CFCl_3$ $\delta$ = 0.0 ppm). FTIR spectra were recorded on a Thermo-Nicolet iS10 FTIR spectrometer. Samples were prepared as $C_6D_6$, $C_6D_{12}$, and $CDCl_3$ solutions injected into a ThermoFisher solution cell equipped with KBr windows or as KBr pellets. For solution FTIR spectra, solvent peaks were digitally subtracted from all spectra by comparison with an authentic spectrum obtained immediately prior to that of the sample. The following abbreviations were used for the intensities and characteristics of important IR absorption bands: vs = very strong, s = strong, m = medium, w = weak, vw = very weak; b = broad, vb = very broad, sh = shoulder. High resolution mass spectrometry (HRMS) was performed using an Agilent 6230 ESI-TOFMS instrument running in positive ion mode. Combustion analyses were performed by Robertson Microlit Laboratories of Madison, NJ (U.S.A.). Full details for the synthesis and characterization of isocyanide ligands $CNAr^{Clips2}$ and $CNAr^{DArF}$ are provided below. Full experimental details for all other compounds are provided in the Supporting Information.

**Synthesis of $IAr^{Clips2}$.** To 100 mL of $CH_2Cl_2$ was added solid 2,6-(2,6-$Cl_2C_6H_3$)$_2C_6H_3I$ (8.500 g, 17.2 mmol). To this solution was sequentially added 20 equivalent portions each of $AlCl_3$ (2.747 g, 20.6 mmol, 1.2 equiv) and 2-methyl-2-chloropropane (31.7 g, 0.345 mol, 20.0 equiv). The addition of $AlCl_3$ was followed by the addition of 2-methyl-2-chloropropane 1 min later, followed by a 3 min interval after which both regents were added again with the 1 min separation. This sequence was continued until all of the $AlCl_3$ and 2-methyl-2-chloropropane was added. Following the last addition, the resulting purple $CH_2Cl_2$ solution was cooled to 0 °C and 100 mL of a saturated aqueous solution of NaCl was added. The reaction mixture was allowed to stir for 20 min. The organic and aqueous layers were then separated, and the organic layer was washed with $CH_2Cl_2$ (3 × 50 mL). The combined $CH_2Cl_2$ extracts were stirred over $MgSO_4$, filtered and dried in vacuo, affording a brown semisolid that was used without further purification. Yield: 7.00 g, 12.72 mmol, 73%. $^1H$ NMR (400.1 MHz, $C_6D_6$, 20 °C): $\delta$ = 7.27 (s, 2H, *m*-Ph), 7.08 (d, 4H, $J$ = 8 Hz, *m*-Clips), 6.62 (t, 2H, $J$ = 8 Hz, *p*-Clips), 1.11 (s, 9H, C($CH_3$)$_3$) ppm. $^{13}C\{^1H\}$ NMR (100.6 MHz, $C_6D_6$, 20 °C): $\delta$ = 152.6, 143.8, 143.2, 135.8, 135.7, 127.4, 127.3, 126.5, 34.8 (*C*($CH_3$)$_3$), 31.0 (C(*C*H$_3$)$_3$) ppm. FTIR ($C_6D_6$, KBr windows): 2966 (s), 2907 (w), 2871 (w), 1590 (w), 1559 (m), 1477 (w), 1430 (vs), 1410 (m), 1391 (m), 1245 (m), 1193 (m), 1091 (w), 1007 (m), 813 (m), 791 (s), 777 (s), 724 (w) $cm^{-1}$. Anal. Calcd. for $C_{22}H_{17}Cl_4I$: C, 48.04; H, 3.12; N, 0.00. Found: C, 47.71; H, 2.97; N, < 0.02.

**Synthesis of $LiAr^{Clips2}$.** To a thawing *n*-pentane solution of $IAr^{Clips2}$ (7.00 g, 12.7 mmol, 400 mL) was added 8.35 mL of 1.6 M *n*-butyllithium in hexanes (13.3 mmol, 1.05 equiv.), and the mixture was allowed to stir for 1 h. The reaction mixture was concentrated to a volume of 100 mL, filtered, and the resulting white solid was washed with thawing *n*-pentane (2 × 50 mL) before being dried in vacuo. Yield: 5.49 g, 12.7 mmol, 99%. $^1H$ NMR (400.1 MHz, $C_6D_6$, 20 °C): $\delta$ = 7.13 (s, 2H, *m*-Ph), 6.94 (d, 4H, $J$ = 8 Hz, *m*-Clips), 6.52 (t, 2H, $J$ = 8 Hz, *p*-Clips), 1.24 (s, 9H, C($CH_3$)$_3$) ppm. $^{13}C\{^1H\}$ NMR (100.6 MHz, $C_6D_6$, 20 °C): $\delta$ = 149.9, 148.6, 146.1, 137.0, 135.6, 134.0, 129.9, 129.4, 34.5 (*C*($CH_3$)$_3$), 31.4 (C(*C*H$_3$)$_3$) ppm. Anal. Calcd. for $C_{22}H_{17}LiCl_4$: C, 61.43; H, 3.98; N, 0.00. Found: C, 59.60; H, 3.93; N, <0.02.

**Synthesis of $N_3Ar^{Clips2}$.** To an $Et_2O$ solution of $LiAr^{Clips2}$ (5.45 g, 12.6 mmol, 400 mL) was added an $Et_2O$ solution of $TosN_3$ (2.624 g, 13.3 mmol, 1.05 equiv, 20 mL). The opaque yellow solution was allowed to stir at room temperature for 2 h, after which 100 mL of $H_2O$ was added and the reaction mixture was stirred for an additional 20 min. The organic and aqueous layers were separated, and the aqueous layer was washed with $Et_2O$ (3 × 80 mL). The combined $Et_2O$ extracts were stirred over $MgSO_4$, filtered, and dried in vacuo, affording $N_3Ar^{Clips2}$ as a yellow solid that was used without further purification. Yield: 5.47 g, 11.8 mmol, 93%. $^1H$ NMR (400.1 MHz, $C_6D_6$, 20 °C): $\delta$ = 7.36 (s, 2H, *m*-Ph), 7.28 (d, 4H, $J$ = 8 Hz, *m*-Clips), 6.90 (t, 2H, $J$ = 8 Hz, *p*-Clips), 1.24 (s, 9H, C($CH_3$)$_3$) ppm. $^{13}C\{^1H\}$ NMR (100.6 MHz, $C_6D_6$, 20 °C): $\delta$ = 149.0, 137.0, 136.3, 133.8, 131.2, 130.2, 128.9, 128.2, 34.7 (*C*($CH_3$)$_3$), 31.2 (C(*C*H$_3$)$_3$) ppm. FTIR ($C_6D_6$, KBr windows): $\nu_{N3}$ = 2110 (vs) $cm^{-1}$, also, 2965 (s), 2904 (m), 2869 (m), 1557 (s), 1466 (m), 1430 (s), 1396 (w), 1363 (w), 1327 (w), 1244 (s), 1147 (w), 1091 (w), 1027 (w), 889 (w), 841 (w), 744 (w), 719 (w) $cm^{-1}$. Anal. Calcd. for $C_{22}H_{17}N_3Cl_4$: C, 56.80; H, 3.68; N, 9.04. Found: C, 56.52; H, 3.71; N, 8.78.

**Synthesis of $NH_2Ar^{Clips2}$.** Under an $N_2$ atmosphere, an $Et_2O$ solution of $N_3Ar^{Clips2}$ (5.47 g, 11.8 mmol, 50 mL) was added dropwise via a pressure-equalizing addition funnel to an $Et_2O$ slurry of $LiAlH_4$ (1.0 g, 35.4 mmol, 3.0 equiv, 150 mL) over 10 min. The reaction mixture was allowed to stir for 1 h and then cooled to 0 °C. To the cooled solution was added 70 mL of $H_2O$ dropwise via a pressure-equalizing addition funnel over the course of 20 min. The reaction was allowed to warm to room temperature, after which it was neutralized with 35 mL of 1 M aqueous HCl. The organic layer was decanted from the aqueous layer, and the aqueous layer was then washed with $Et_2O$ (2 × 50 mL). The combined $Et_2O$ extracts were stirred over $MgSO_4$, filtered, and dried in vacuo, affording $NH_2Ar^{Clips2}$ as a colorless solid. Yield: 5.16 g, 11.8 mmol, 99%. $^1H$ NMR (400.1 MHz, $C_6D_6$, 20 °C): $\delta$ = 7.21 (s, 2H, *m*-Ph), 7.08 (d, 4H, $J$ = 8 Hz, *m*-Clips), 6.59 (t, 2H, $J$ = 8 Hz, *p*-Clips), 2.96 (s, 2H, N$H_2$), 1.23 (s, 9H, C($CH_3$)$_3$) ppm. $^{13}C\{^1H\}$ NMR (100.6 MHz, $C_6D_6$, 20 °C): $\delta$ = 141.2, 139.3, 137.9, 136.7, 129.6, 128.5, 127.6, 123.4, 34.2 (*C*($CH_3$)$_3$), 31.7 (C(*C*H$_3$)$_3$) ppm. FTIR ($C_6D_6$, KBr windows): $\nu_{NH}$ = 3472 (m) and 3392 (m) $cm^{-1}$, also 2964 (s), 2903 (w), 2866 (w), 1612 (m), 1597 (w), 1554 (s), 1480 (m), 1443 (w), 1428 (s), 1330 (m), 1258 (m), 1241 (m), 1189 (m), 814 (w), 789 (s) $cm^{-1}$. Anal. Calcd. for $C_{22}H_{19}NCl_4$: C, 60.16; H, 4.36; N, 3.19. Found: C, 59.91; H, 4.28; N, 3.14.

**Synthesis of $HC(O)NHAr^{Clips2}$.** Neat acetic anhydride (9.65 g, 94.5 mmol, 8 equiv) was cooled to 0 °C under an $N_2$ atmosphere and formic acid (5.44 g, 118.0 mmol, 10 equiv) was added via syringe over 20 min. The resulting colorless solution was heated for 3 h at 60 °C and then allowed to cool to room temperature. To this mixture containing formyl acetic anhydride, was added a THF solution of $NH_2Ar^{Clips2}$ (5.16 g, 11.8 mmol, 1 equiv, 100 mL), and the reaction mixture was allowed to stir for 12 h. All volatile materials were then removed under reduced pressure. The resultant pale-yellow residue was then slurried in cold hexanes (−30 °C, 50 mL) and filtered to afford $HC(O)NHAr^{Clips2}$ as a colorless solid, which was dried in vacuo and collected. Yield: 4.6 g, 9.85 mmol, 83%. $^1H$ NMR analysis at 20 °C of $HC(O)NHAr^{Clips2}$ as isolated above indicated a 4:1 mixture of trans- and cis- isomers (see the Supporting Information for full details). This isomeric mixture was used in the subsequent dehydration step without separation. Spectroscopic data for the trans-isomer: $^1H$ NMR (400.1 MHz, $C_6D_6$, 20 °C): $\delta$ = 8.23 (d, 1H, $J$ = 11 Hz, NHC(O)*H*), 7.32 (s, 2H, *m*-Ph), 7.21 (d, 1H, $J$ = 11 Hz, N*H*C(O)H), 6.95 (d, 4H, $J$ = 8 Hz, *m*-Clips), 6.51 (t, 2H, $J$ = 8 Hz, *p*-Clips), 1.11 (s, 9H, C($CH_3$)$_3$) ppm. $^{13}C\{^1H\}$ NMR (100.6 MHz, $C_6D_6$, 20 °C): $\delta$ = 162.6 (*H*C(O)NH), 150.9, 137.0, 135.4, 134.7, 130.2, 130.1, 129.5, 128.7, 34.7 (*C*($CH_3$)$_3$), 31.1 (C(*C*H$_3$)$_3$) ppm. Spectroscopic data for cis-isomer: $^1H$ NMR (400.1 MHz, $C_6D_6$, 20 °C): $\delta$ = 7.43 (s, 2H, *m*-Ph), 7.07 (d, 4H, $J$ = 8 Hz, *m*-Clips), 7.05 (s, 1H, *H*C(O)NH), 6.59 (t, 2H, $J$ = 8 Hz, *p*-Clips), 6.14 (s, 1H, $J$ = 8 Hz, HC(O)N*H*), 1.17 (s, 9H, C($CH_3$)$_3$) ppm. $^{13}C\{^1H\}$ NMR (100.6 MHz, $C_6D_6$, 20 °C): $\delta$ = 157.7 (*H*C(O)NH), 150.5, 138.1, 135.9, 135.3, 131.0, 130.7, 129.5, 34.8 *C*($CH_3$)$_3$, 31.2 C($CH_3$)$_3$ ppm. FTIR isomeric mixture ($C_6D_6$, KBr windows): $\nu_{NH}$ = 3385 (w) $cm^{-1}$, $\nu_{CO}$ = 1702 (vs b) $cm^{-1}$, also 3079 (w), 2966 (s), 2906 (w), 1484 (w), 1460 (w), 1445 (w), 1429 (s), 1397 (m), 1245 (m), 1193 (m), 1092 (w), 790 (s) $cm^{-1}$. HRMS isomeric mixture (ESI, Acetone): $m/z$ Found =462.39 $[M+H]^+$. Anal. Calcd. for $C_{23}H_{19}NOCl_4$ (bulk sample, isomeric mixture): C, 59.13; H, 4.10; N, 3.00. Found: C, 58.34; H, 3.83; N, 2.89.

**Synthesis of $CNAr^{Clips2}$.** To a $CH_2Cl_2$ solution of $HC(O)NHAr^{Clips2}$ (4:1 mixture of trans/cis isomers; 4.60 g, 9.85 mmol, 100 mL) was added diisopropylamine (13.95 g, 137 mmol, 14.0 equiv). The solution was cooled to 0 °C under an $N_2$ atmosphere, and $POCl_3$

(4 mL, 6.64 g, 43.3 mmol, 4.4 equiv) was added dropwise via syringe. The resulting mixture was allowed to stir for 12 h, after which 70 mL of an aqueous 0.9 M $Na_2CO_3$ was added. After an additional 1 h of stirring, the organic and aqueous layers were separated, and the aqueous layer was washed with $CH_2Cl_2$ (3 × 70 mL). The combined organic extracts were stirred over $MgSO_4$, filtered, and dried in vacuo. The resulting residue was slurried in cold acetonitrile (40 mL, 0 °C), filtered, and dried in vacuo to afford isocyanide $CNAr^{Clips2}$ as a colorless solid. Yield: 3.80 g, 8.45 mmol, 86%. $^1$H NMR (400.1 MHz, $C_6D_6$, 20 °C): $\delta$ = 7.33 (s, 2H, *m*-Ph), 6.99 (d, 4H, $J$ = 8 Hz, *m*-Clips), 6.53 (t, 2H, $J$ = 8 Hz, *p*-Clips), 1.07 (s, 9H, $C(CH_3)_3$) ppm. $^{13}C\{^1H\}$ NMR (100.6 MHz, $C_6D_6$, 20 °C): $\delta$ = 172.0 ($C{\equiv}N$), 153.0, 136.1, 135.5, 135.3, 130.6, 128.4, 128.0, 35.1 $C(CH_3)_3$, 30.9 $C(CH_3)_3$ ppm. FTIR (KBr pellet): $\nu_{CN}$ = 2132 (s) cm$^{-1}$, also 2965 (s), 1599 (w), 1558 (m), 1424 (vs), 1399 (w), 1366 (w), 1247 (w), 1193 (m), 1091 (w), 1027 (w), 889 (w), 781 (vs), 651 (w), and 622 (w) cm$^{-1}$. FTIR ($C_6D_6$, KBr windows): $\nu_{CN}$ = 2119 (s) cm$^{-1}$, also 2968 (s b), 1598 (w), 1557 (w), 1428 (m), 1400 (w), 1247 (m), 791 (s), 779 (s), 742 (w), 707 (w), 654 (w), 625 (w) cm$^{-1}$. Anal. Calcd. for $C_{23}H_{17}NCl_4$: C, 61.50; H, 3.81; N, 3.12. Found: C, 61.32; H, 3.82; N, 2.97.

**Synthesis of $H_2NAr^{DArF2}$.** A resealable ampule was charged with 2,6-dibromoaniline (0.915 g, 3.60 mmol), 3,5-bis(trifluoromethyl)-phenylboronic acid (2.04 g, 8.00 mmol, 2.2 equiv), $Na_2CO_3$ (1.56 g, 15.0 mmol, 4.4 equiv) and placed under an $N_2$ atmosphere. A toluene (25 mL) solution containing $Pd_2(dba)_3$ (0.017 g, 0.018 mmol, 0.5 mol %) and $PPh_3$ (0.009 g, 0.036 mmol, 1 mol %) was then added, followed by $H_2O$ (5 mL) and EtOH (10 mL). The ampule was sealed and heated at 90 °C for 16 h. The reaction mixture was cooled to room temperature and filtered through a medium porosity frit packed with Celite. Water (20 mL) was added to the filtrate and 1 M aqueous HCl was then added to achieve a pH of 7.0. The aqueous and organic phases were then separated, and the aqueous layer was then washed with $Et_2O$ (3 × 10 mL). The combined organic phases were dried over $MgSO_4$ and then all volatile materials were removed by rotary evaporation. The resulting yellow oil was purified by column chromatography (silica gel) using hexanes to elute the principal contaminants and then 0.5% EtOAc in hexanes to elute $H_2NAr^{DArF2}$. Fractions containing $H_2NAr^{DArF2}$ were combined and volatile materials were removed by rotary evaporation to afford a colorless solid. Yield: 1.206 g, 2.30 mmol, 65%. $^1$H NMR (499.8 MHz, $C_6D_6$, 20 °C): $\delta$ = 7.76 (s, 2H, *p*-ArF), 7.67 (s, 4H, *o*-ArF), 6.64 (m, 3H, *p*-Ph + *m*-Ph), 2.71 (s, 2H, $NH_2$) ppm. $^{13}C\{^1H\}$ NMR (125.7 MHz, $C_6D_6$, 20 °C): $\delta$ = 141.9, 140.7, 132.5 (q, $^2J_{C-F}$ = 33 Hz, *m*-ArF), 131.3, 129.7, 125.1, 123.8 (q, $^1J_{C-F}$ = 273 Hz, $CF_3$), 121.4 (septet, $^3J_{C-F}$ = 4 Hz, *p*-ArF), 119.3 ppm. $^{19}$F NMR (470.6 MHz, $C_6D_6$, 20 °C): $\delta$ = −63.38 (s, $CF_3$) ppm. FTIR ($C_6D_6$, KBr windows): $\nu_{NH}$ = 3487 (w), 3398 (m) cm$^{-1}$, also 3065 (w), 2962 (vw), 2915 (w), 1805 (m), 1783 (m), 1675 (m), 1616 (s), 1377 (vs), 1283 (vs), 1211 (s), 1178 (vs), 1142 (vs), 906 (s), 845 (m), 751 (m), 709 (m), 681 (m), 637 (m) cm$^{-1}$. Anal. Calcd. For $C_{22}H_{11}F_{12}N$: C, 51.08; H, 2.14; N, 2.71. Found: C, 50.83; H, 2.28; N, 2.78.

**Synthesis of $HC(O)NHAr^{DArF2}$.** Neat acetic anhydride (5.9 g, 58.0 mmol, 20 equiv) was cooled to 0 °C under an $N_2$ atmosphere, and formic acid (3.33 g, 73.0 mmol, 25 equiv) was added via syringe over 20 min. The resulting colorless solution was heated for 3 h at 60 °C and then allowed to cool to room temperature. This mixture now containing formyl acetic anhydride was then cooled to room temperature and added, via syringe, to a toluene solution of $H_2NAr^{DArF2}$ (1.01 g, 1.95 mmol, 50 mL). The resulting mixture was stirred for 16 h. All volatile materials were then removed by rotary evaporation to afford a colorless solid that was used without further purification. Yield: 0.880 g, 1.60 mmol, 82%. $^1$H NMR (499.8 MHz, $C_6D_6$, 20 °C): $\delta$ = 7.76 (s, 2H, *p*-ArF), 7.59 (s, 4H, *o*-ArF), 6.96 (s, 1H, *H*C(O)NH), 6.91 (t, 1H, $J$ = 8 Hz, *p*-Ph), 6.72 (d, 2H, $J$ = Hz, *m*-Ph), 4.60 (s, 1H, HC(O)N*H*) ppm. $^{13}C\{^1H\}$ NMR (125.7 MHz, $C_6D_6$, 20 °C): $\delta$ = 159.1 ($HC(O)NHAr^{ArF2}$), 141.5, 138.1, 131.9 (q, $^2J_{C-F}$ = 33 Hz, *m*-ArF), 130.9, 130.4, 129.4, 127.5, 123.8 (q, $^1J_{C-F}$ = 273 Hz, $CF_3$), 121.6 (septet, $^3J_{C-F}$ = 4 Hz, *p*-ArF) ppm. $^{19}$F NMR (470.6 MHz, $C_6D_6$, 20 °C): $\delta$ = −63.34 (s, $CF_3$) ppm. FTIR ($C_6D_6$, KBr windows): $\nu_{NH}$ = 3367 (w), $\nu_{CO}$ = 1707 (s) cm$^{-1}$; also 2917 (w), 2851 (w), 1680 (s), 1374 (s), 1277 (vs), 1208 (sh), 1183 (vs), 1138 (vs), 903 (m), 850 (m), 800 (m), 725 (m), 705 (w), 633 (w) cm$^{-1}$. Anal. Calcd. for $C_{23}H_{11}F_{12}NO$: C, 50.66; H, 2.03; N, 2.57. Found: C, 50.77; H, 1.84; N, 2.66.

**Synthesis of $CNAr^{DArF2}$.** Diisopropylamine ($HN(i\text{-}Pr)_2$; 0.520 g, 5.13 mmol, 3.4 equiv) was added, via syringe, to a $CH_2Cl_2$ solution of $HC(O)NHAr^{DArF2}$ (0.800 g, 1.50 mmol, 60 mL). The resulting mixture was cooled to 0 °C and $POCl_3$ (0.450 g, 2.93 mmol, 1.95 equiv) was added by syringe. The reaction mixture was allowed to warm slowly to room temperature and then stirred for 16 h. Aqueous $Na_2CO_3$ (1.5 M, 40 mL) was then added, and the resulting mixture stirred for 1 h. The organic and aqueous layers were separated, and the aqueous layer was washed with $CH_2Cl_2$ (3 × 20 mL). The combined organic layers were dried over $MgSO_4$ and then all volatile materials were removed by rotary evaporation. The resulting solid was dissolved in a minimal amount of MeCN and cooled to −40 °C to produce a colorless precipitate. Cold filtration of the mixture then afforded $CNAr^{DArF2}$ a colorless solid. Yield: 0.400 g, 0.75 mmol, 51%. $^1$H NMR (499.8 MHz, $C_6D_6$, 20 °C): $\delta$ = 7.83 (s, 2H, *p*-ArF), 7.75 (s, 4H, *o*-ArF), 6.86 (t, 1H, $J$ = 8 Hz, *p*-Ph), 6.62 (d, 2H, $J$ = 8 Hz, *m*-Ph) ppm. $^{13}C\{^1H\}$ NMR (125.7 MHz, $C_6D_6$, 20 °C): $\delta$ = 175.4 (CNR), 139.0, 136.8, 132.2 (q, $^2J_{C-F}$ = 34 Hz, *m*-ArF), 130.4, 129.7, 129.6, 127.5, 123.6 (q, $^1J_{C-F}$ = 273 Hz, $CF_3$), 122.6 (septet, $J_{C-F}$ = 4 Hz, *p*-ArF) ppm. $^{19}$F NMR (470.4 MHz, $C_6D_6$, 20 °C): $\delta$ = −63.25 (s, $CF_3$) ppm. FTIR ($C_6D_6$, KBr windows): $\nu_{CN}$ = 2112 (s) cm$^{-1}$ also, 3087 (w), 3056(w), 2956 (w), 2923 (w), 1624 (w), 1483 (w), 1459 (m), 1372 (vs), 1279 (vs), 1250 (m), 1182 (vs), 1142 (vs), 1110 (m), 1073 (w), 1060 (w), 900 (m), 847 (w), 803 (m), 749 (m), 683 (m), 637 (w) cm$^{-1}$. FTIR ($C_6D_6$, KBr Pellet): $\nu_{CN}$ = 2119 (s) cm$^{-1}$ also, 3097 (m), 2967 (w), 2929 (w), 1627 (m), 1465 (m), 1374 (vs), 1280, (vs), 1250 (s), 1193 (s), 1169 (s), 1118 (vs), 1069 (m), 908 (s), 850 (m), 747 (s), 708 (s), 683 (s), 633 (m), 545 (w) cm$^{-1}$. Anal. Calcd. for $C_{23}H_9F_{12}N$: C, 52.39; H, 1.72; N, 2.66. Found: C, 52.07; H, 1.65; N, 2.70.

**Crystallographic Structure Determinations.** Single crystal X-ray structure determinations were carried out at low temperature on Bruker Platform or Kappa Diffractometers equipped with either Mo or Cu radiation sources and Bruker APEX, APEX-II, and Photon 100 area detectors. All structures were solved via direct methods with SIR 2004[102] and refined by full-matrix least-squares procedures utilizing SHELXL-2013.[103] Crystallographic data collection and refinement information are listed in Supporting Information, Table S1. The crystallographic routine SQUEEZE[104] was used to account for disordered solvent of cocrystallization in the crystal structures of $\mathbf{1}^{Mes}$, $\mathbf{3}^{Clips}$, and $\mathbf{4}^{Clips}$. The crystal structure of $\mathbf{4}^{DArF}$ contains a two-site positional disorder of the $\eta^6$-$C_6H_6$ ligand. The disorder was modeled such that the $\eta^6$-$C_6H_6$ ligands are present at 50% occupancy at each of the two sites. The crystal structure of $\mathbf{1}^{Mes}$ exhibits a 2% whole-molecule disorder. Only the metal center was modeled because of the low percentage. The crystal structure of $\mathbf{8}^{DArF}$ exhibits whole-molecule disorder of the ligand framework, which was modeled. All disorder was modeled and refined using standard crystallographic techniques.

## ■ ASSOCIATED CONTENT

### Ⓢ Supporting Information

Experimental procedures, spectral data, and results of crystallographic structure determinations (PDF and CIF). This material is available free of charge via the Internet at http://pubs.acs.org.

## ■ AUTHOR INFORMATION

### Corresponding Author

*E-mail: jsfig@ucsd.edu.

### Notes

The authors declare no competing financial interest.

## ■ ACKNOWLEDGMENTS

We are grateful to the U.S. Department of Energy (DE-SC0008058) and Research Corporation (through a Cottrell Scholar Award to J.S.F) for support of this work. A.E.C. acknowledges support from the U.S. National Science Foundation through a Graduate Research Fellowship. D.S.R is grateful to the California Institute of Telecommunications and Information Technology (CalIT$^2$) for an undergraduate summer research scholarship. We thank Prof. John D. Protasiewicz for insightful comments and for suggesting the use of 2,6-dichlorophenyl-substituted *m*-terphenyls in isocyanide chemistry. We also acknowledge Joshua Day for experimental assistance.

## ■ REFERENCES

(1) Twamley, B.; Haubrich, S. T.; Power, P. P. *Adv. Organomet. Chem.* **1999**, *44*, 1−65.
(2) Power, P. P. *Chem. Rev.* **1999**, *99*, 3463−3504.
(3) Clyburne, J. A. C.; McMullen, N. *Coord. Chem. Rev.* **2000**, *210*, 73−99.
(4) Robinson, G. H. *Acc. Chem. Res.* **1999**, *32*, 773−782.
(5) Robinson, G. H. *Chem. Commun.* **2000**, 2175−2181.
(6) Power, P. P. *Chem. Commun.* **2003**, 2091−2101.
(7) Power, P. P. *Organometallics* **2007**, *26*, 4362−4372.
(8) Rivard, E.; Power, P. P. *Inorg. Chem.* **2007**, *46*, 10047−10064.
(9) Kays, D. L. *Organomet. Chem.* **2010**, *36*, 56−76.
(10) Kays, D. L. *Dalton Trans.* **2011**, *40*, 769−778.
(11) Power, P. P. *Chem. Rev.* **2012**, *112*, 3482−3507.
(12) Stanciu, C.; Olmstead, M. M.; Phillips, A. D.; Stender, M.; Power, P. P. *Eur. J. Inorg. Chem.* **2003**, 3495−3500.
(13) Hill, J. E.; Fanwick, P. E.; Rothwell, I. P. *Organometallics* **1990**, *9*, 2211−2213.
(14) Hill, J. E.; Fanwick, P. E.; Rothwell, I. P. *Organometallics* **1991**, *10*, 15−16.
(15) Hill, J. E.; Balaich, G. J.; Fanwick, P. E.; Rothwell, I. P. *Organometallics* **1991**, *10*, 3428−3430.
(16) Ni, C.; Power, P. P. *Chem. Commun.* **2009**, 5543−5545.
(17) Ellison, J. J.; Ruhlandt-Senge, K.; Power, P. P. *Angew. Chem., Int. Ed. Engl.* **1994**, *33*, 1178−1180.
(18) Buyuktas, B. S.; Olmstead, M. M.; Power, P. P. *Chem. Commun.* **1998**, 1689−1690.
(19) Rekken, B. D.; Brown, T. M.; Olmstead, M. M.; Fettinger, J. C.; Power, P. P. *Inorg. Chem.* **2013**, *52*, 3054−3062.
(20) Rekken, B. D.; Brown, T. M.; Fettinger, J. C.; Lips, F.; Tuononen, H. M.; Herber, R. H.; Power, P. P. *J. Am. Chem. Soc.* **2013**, *135*, 10134−10148.
(21) Merrill, W. A.; Steiner, J.; Betzer, A.; Nowik, I.; Herber, R.; Power, P. P. *Dalton Trans.* **2008**, 5905−5910.
(22) Li, J.; Song, H.; Cui, C.; Cheng, J.-P. *Inorg. Chem.* **2008**, *47*, 3468−3470.
(23) Ni, C.; Rekken, B.; Fettinger, J. C.; Long, G. J.; Power, P. P. *Dalton Trans.* **2009**, 8349−8355.
(24) Merrill, W. A.; Stich, T. A.; Brynda, M.; Yeagle, G. J.; Fettinger, J. C.; De Hont, R.; Reiff, W.; Schulz, C. E.; Britt, R. D.; Power, P. P. *J. Am. Chem. Soc.* **2009**, *131*, 12693−12702.
(25) Ni, C.; Fettinger, J. C.; Long, G. J.; Power, P. P. *Inorg. Chem.* **2009**, *48*, 2443−2448.
(26) Merrill, W. A.; Wright, R. J.; Stanciu, C. S.; Olmstead, M. M.; Fettinger, J. C.; Power, P. P. *Inorg. Chem.* **2010**, *49*, 7097−7105.
(27) Bryan, A. M.; Merill, W. A.; Reiff, W. M.; Fettinger, J. C.; Power, P. P. *Inorg. Chem.* **2012**, *51*, 3366−3373.
(28) Boynton, J. N.; Merrill, W. A.; Reiff, W. A.; Fettinger, J. C.; Power, P. P. *Inorg. Chem.* **2012**, *51*, 3212−3219.
(29) Boynton, J. N.; Guo, J.- D.; Fettinger, J. C.; Melton, C. E.; Nagase, S.; Power, P. P. *J. Am. Chem. Soc.* **2013**, *135*, 10720−10728.
(30) Gavenonis, J.; Tilley, T. D. *J. Am. Chem. Soc.* **2002**, *124*, 8536−8537.
(31) Gavenonis, J.; Tilley, T. D. *Organometallics* **2002**, *21*, 5549−5563.
(32) Hagadorn, J. R.; Que, L., Jr.; Tolman, W. B.; Prisecaru, I.; Munck, E. *J. Am. Chem. Soc.* **1999**, *121*, 9760−9761.
(33) Hagadorn, J. R.; Que, L., Jr.; Tolman, W. B. *Inorg. Chem.* **2000**, *39*, 6086−6090.
(34) Carson, E. C.; Lippard, S. J. *J. Am. Chem. Soc.* **2004**, *126*, 3412−3413.
(35) Yoon, S.; Lippard, S. J. *J. Am. Chem. Soc.* **2005**, *127*, 8386−8397.
(36) Carson, E. C.; Lippard, S. J. *Inorg. Chem.* **2006**, *45*, 828−836.
(37) Klein, D. P.; Young, V. G., Jr.; Tolman, W. B.; Que, L., Jr. *Inorg. Chem.* **2006**, *45*, 8006−8008.
(38) Carson, E. C.; Lippard, S. J. *Inorg. Chem.* **2006**, *45*, 837−848.
(39) Fox, B. J.; Sun, Q. Y.; DiPasquale, A. G.; Fox, A. R.; Rheingold, A. L.; Figueroa, J. S. *Inorg. Chem.* **2008**, *47*, 9010−9020.
(40) Ditri, T. B.; Fox, B. J.; Moore, C. E.; Rheingold, A. L.; Figueroa, J. S. *Inorg. Chem.* **2009**, *48*, 8362−8375.
(41) Weidemann, N.; Margulieux, G. W.; Moore, C. E.; Rheingold, A. L.; Figueroa, J. S. *Inorg. Chim. Acta* **2010**, *354*, 238−245.
(42) Stewart, M. A.; Moore, C. E.; Ditri, T. B.; Labios, L. A.; Rheingold, A. L.; Figueroa, J. S. *Chem. Commun.* **2010**, 406−408.
(43) Ditri, T. B.; Moore, C. E.; Rheingold, A. L.; Figueroa, J. S. *Inorg. Chem.* **2011**, *50*, 10448−10459.
(44) Margulieux, G. M.; Weidemann, N.; Lacy, D. C.; Moore, C. E.; Rheingold, A. L.; Figueroa, J. S. *J. Am. Chem. Soc.* **2010**, *132*, 5033−5035.
(45) Fox, B. J.; Millard, M. D.; DiPasquale, A. G.; Rheingold, A. L.; Figueroa, J. S. *Angew. Chem., Int. Ed.* **2009**, *48*, 3473−3477.
(46) Emerich, B. M.; Moore, C. E.; Fox, B. J.; Rheingold, A. L.; Figueroa, J. S. *Organometallics* **2011**, *30*, 2598−2608.
(47) Labios, L. A.; Millard, M. D.; Rheingold, A. L.; Figueroa, J. S. *J. Am. Chem. Soc.* **2009**, *131*, 11318−11319.
(48) Carpenter, A. E.; Margulieux, G. W.; Millard, M. D.; Moore, C. E.; Weidemann, N.; Rheingold, A. L.; Figueroa, J. S. *Angew. Chem., Int. Ed.* **2012**, *51*, 9412−9416.
(49) Nguyen, T.; Merrill, W. A.; Ni, C.; Lei, H.; Fettinger, J. C.; Ellis, B. D.; Long, G. J.; Brynda, M.; Power, P. P. *Angew. Chem., Int. Ed.* **2008**, *47*, 9115−9117.
(50) Lei, H.; Ellis, B. D.; Ni, C.; Grandiean, F.; Long, G. J.; Power, P. P. *Inorg. Chem.* **2008**, *47*, 10205−10207.
(51) Bishop, P. T.; Dilworth, J. R.; Nicholson, T.; Zubieta, J. *J. Chem. Soc., Dalton Trans.* **1991**, 385−392.
(52) Dilworth, J. R.; Zheng, Y.; Lu, S.; Wu, Q. *Inorg. Chim. Acta* **1992**, *194*, 99−103.
(53) Buyuktas, B. S.; Olmstead, M. M.; Power, P. P. *Chem. Commun.* **1998**, 1689−1690.
(54) Ohki, Y.; Takikawa, Y.; Sadohara, H.; Kesenheimer, C.; Engendahl, B.; Kapatina, E.; Tatsumi, K. *Chem.—Asian J.* **2008**, *3*, 1625−1635.
(55) Kerschner, J. L.; Rothwell, I. P.; Huffman, J. C.; Streib, W. E. *Organometallics* **1988**, *7*, 1871−1873.
(56) Kerschner, J. L.; Torres, E. M.; Fanwick, P. E.; Rothwell, I. P.; Huffman, J. C. *Organometallics* **1989**, *8*, 1424−1431.
(57) Lockwood, M. A.; Fanwick, P. E.; Rothwell, I. P. *Organometallics* **1997**, *16*, 3574−3575.
(58) Lentz, M. R.; Vilardo, J. S.; Lockwood, M. A.; Fanwick, P. E.; Rothwell, I. P. *Organometallics* **2004**, *23*, 329−343.
(59) Buster, B.; Diaz, A. A.; Graham, T.; Khan, R.; Khan, M.; Powell, D. R.; Welmschulte, R. J. *Inorg. Chim. Acta* **2009**, *362*, 3465−3474.
(60) Ni, C.; Long, G. J.; Power, P. P. *Organometallics* **2009**, *28*, 5012−5016.
(61) Pasynkiewicz, S.; Giezyński, R.; Dzierzgowski, S. *J. Organomet. Chem.* **1973**, *54*, 203−205.
(62) Adedeji, F. A.; Lalage, D.; Brown, S.; Connor, J. A.; Leung, M. L.; Paz-Andrade, I. M.; Skinner, H. A. *J. Organomet. Chem.* **1975**, *97*, 221−228.
(63) Klabunde, K. J.; Anderson, B. B.; Bader, M.; Radonovich, L. J. *J. Am. Chem. Soc.* **1978**, *100*, 1313−1314.

(64) Muetterties, E. L.; Bleeke, J. R.; Sievert, A. C. *J. Organomet. Chem.* **1979**, *178*, 197−216.
(65) Sievert, A. C.; Muetterties, E. L. *Inorg. Chem.* **1981**, *20*, 489−501.
(66) Muetterties, E. L.; Bleeke, J. R.; Wucherer, E. J. *Chem. Rev.* **1982**, *82*, 499−525.
(67) Nolan, S. P.; Lopez de la Vega, R.; Hoff, C. D. *Organometallics* **1986**, *5*, 2529−2537.
(68) Mukerjee, S. L.; Lang, R. F.; Ju, T.; Kiss, G.; Hoff, C. D.; Nolan, S. P. *Inorg. Chem.* **1992**, *31*, 4885−4889.
(69) Schroeter, K.; Wesendrup, R.; Schwarz, H. *Eur. J. Org. Chem.* **1998**, 565−571.
(70) Currently, halo substituents on the flanking ring of an *m*-terphenyl group are limited to two examples reported by Protzsiewicz. See: (a) 3,5-dichloro substitution within the general $Ar^{Mes2}$ framework (i.e., 2,6-(3,5-$Cl_2$-2,4,6-$Me_3C_6$)$_2C_6H_3$) Protzsiewicz, J. D. *J. Chem. Soc., Chem. Commun.* **1995**, 1115−1116. (b) A derivative featuring 2,6-dichlorophenyl groups (i.e., 2,6-(2,6-$Cl_2C_6H_3$)$_2C_6H_3$) Smith, R. C.; Ren, T.; Protasiewicz, J. D. *Eur. J. Inorg. Chem.* **2002**, 2779−2783.
(71) Power has reported transition-metal and main-group complexes featuring *m*-terphenyl groups bearing *para*-fluoro, *para*-chloro, and *para*-trifluoromethyl substituents on the central ring. See; (a) Wolf, R.; Ni, C.; Nguyen, Brynda, M.; Long, G. J.; Sutton, A. D.; Fischer, R. C.; Fettinger, J. C.; Hellman, M.; Pu, L.; Power, P. P. *Inorg. Chem.* **2007**, *46*, 11277−11290. (b) Peng, Y.; Fischer, R. C.; Merrill, W. A.; Fischer, J.; Pu, L.; Ellis, B. D.; Fettinger, J. C.; Herber, R. H.; Power, P. P. *Chem. Sci.* **2010**, *1*, 461−468.
(72) The moniker Clips ostensibly refers to Chloro-isocyanide-with-para-substitution.
(73) For a convenient preparation of Mo($\eta^6$-$C_{10}H_8$)$_2$, see: Pomije, M. K.; Kurth, C. J.; Ellis, J. E.; Barybin, M. V. *Organometallics* **1997**, *16*, 3582−3587.
(74) Kündig, E. P.; Timms, P. T. *J. Chem. Soc., Chem. Commun.* **1997**, 912−913.
(75) Thi, N. P. D.; Spichiger, S.; Paglia, P.; Bernardinelli, G.; Kündig, E. P.; Timms, P. L. *Helv. Chim. Acta* **1992**, *75*, 2593−2607.
(76) Cambridge Structural Database (CSD), version 5.34 (Update 2, Feb. 2013).
(77) Prior to this study, the most acute $C_{iso}$−N−C angles for coordinated, terminal isocyanides were in the range of 126°−135°. See: Shapiro, P. J.; Zehnder, R.; Foo, D. M.; Perrotin, P.; Budzelaar, P. H. M.; Leitch, S.; Twamley, B. *Organometallics* **2006**, *25*, 719−732.
(78) A full account of the spectroscopic and electronic structure features of these geometrically constrained isocyanide ligands will be presented in an upcoming paper.
(79) Perutz, R. N.; Turner, J. J. *J. Am. Chem. Soc.* **1975**, *97*, 4800−4804.
(80) Perutz, R. N.; Turner, J. J. *Inorg. Chem.* **1975**, *14*, 262−270.
(81) Ishikawa, Y.; Kawakami, K. *J. Phys. Chem. A* **2007**, *111*, 9940−9944.
(82) (a) Nishida, H.; Takada, N.; Ycmhmura, M.; Sonoda, T.; Kobayashi, H. *Bull. Chem. Soc. Jpn.* **1984**, *57*, 2600−2604. (b) Brookhart, M.; Grant, B.; Volpe, A. F., Jr *Organometallics* **1992**, *11*, 3920−3922. (c) Taube, R.; Wache, S. *J. Orgonomet. Chem.* **1992**, *428*, 431−442.
(83) Krossing, I.; Raabe, I. *Angew. Chem., Int. Ed.* **2004**, *43*, 2066−2090.
(84) Powell, J.; Lough, A.; Saeed, T. *J. Chem. Soc., Dalton Trans.* **1997**, 4137−4138.
(85) Douglas, T. M.; Molinos, E.; Brayshaw, S. K.; Weller, A. S. *Organometallics* **2007**, *26*, 463−465.
(86) Connor, J. A.; Jones, E. M.; McEwen, G. K.; Lloyd, M. K.; McCleverty, J. A. *J. Chem. Soc., Dalton Trans.* **1972**, 1246−1253.
(87) Johnston, R. F.; Cooper, J. C. *J. Mol. Struct.* **1991**, *236*, 297−307.
(88) Guang, Z.; Janak, K. E.; Figueroa, J. S.; Parkin, G. *J. Am. Chem. Soc.* **2006**, *128*, 5452−5461.
(89) The paramagnetism of $\mathbf{6}^{Clips}$ does not allow for its accurate quantification relative to $\mathbf{1}^{Clips2}$ or **7** by $^1$H NMR spectroscopy. We also presume that molybdenum metal is formed as a byproduct in these thermolysis reactions.
(90) Smith, R. C.; Shah, S.; Urnezius, E.; Protasiewicz, J. D. *J. Am. Chem. Soc.* **2003**, *125*, 40−41.
(91) Essenmacher, G. J.; Treichel, P. M. *Inorg. Chem.* **1977**, *16*, 800−806.
(92) Treichel, P. M.; Mueh, H. J. *Inorg. Chem.* **1977**, *16*, 1167−1169.
(93) Lentz, D. *J. Organomet. Chem.* **1990**, *381*, 205−212.
(94) Lentz, D. *Angew. Chem., Int. Ed. Engl.* **1994**, *33*, 1315−1331.
(95) Lentz, D.; Anibarro, M.; Preugschat, D.; Bertrand, G. *J. Fluor. Chem.* **1998**, *89*, 73−81.
(96) On the basis of electrochemical studies on $[Mn(CNAr)_6]^+$ complexes, Treichel has shown that *p*-tolyl isocyanide is a weaker $\pi$-acid than phenyl isocyanide. Accordingly, *para*-alkyl substituents may generally be expected to attenuate the $\pi$-acceptor properties of aryl isocyanides. See ref 92.
(97) Similarly, the IR spectrum of *mer*-$\mathbf{9}^{Mes}$ gives rise to only two well-resolved $\nu_{CO}$ bands. See the Supporting Information for more details.
(98) Zhou, M.; Andrews, L.; Bauschlicher, C. W., Jr. *Chem. Rev.* **2001**, *101*, 1931−1962.
(99) Pangborn, A. B.; Giardello, M. A.; Grubbs, R. H.; Rosen, R. K.; Timmers, F. J. *Organometallics* **1996**, *15*, 1518−1520.
(100) Arnarego, W. L. F.; Chai, C. L. L. *Purification of Laboratory Chemicals*, 5th ed.; Elsevier: Amsterdam, The Netherlands, 2003.
(101) McElwee-White, L.; Dougherty, D. A. *J. Am. Chem. Soc.* **1984**, *106*, 3466−3474.
(102) Burla, M. C.; Caliandro, R.; Camalli, M.; Carrozzini, B.; Cascarano, G. L.; De Caro, L.; Giacovazzo, C.; Polidori, G.; Spagna, R. *J. Appl. Crystallogr.* **2005**, *38*, 381−388.
(103) Sheldrick, G. M. *Acta Crystallogr.* **2008**, *A64*, 112−122.
(104) van der Sluis, P.; Spek, A. L. *Acta Crystallogr.* **1990**, *A46*, 194−201.